EFFECTS OF COMPATIBILIZER TYPE AND PROCESSING PARAMETERS ON MECHANICAL PROPERTIES OF POLYPROPYLENE-CLAY NANOCOMPOSITES PREPARED BY MELT MIXING

by

M. Bora İşlier

B.S., in M.E., Yıldız Technical University, 2005

Submitted to the Institute for Graduate Studies in
Science and Engineering in partial fulfillment of
the requirements for the degree of
Master of Science

Graduate Program in Mechanical Engineering

Boğaziçi University

2008

ACKNOWLEDGEMENTS

I wish to express my sincere gratitude to my supervisor Asst. Prof. Nuri Ersoy for his supervision, academic support, suggestions and guidance all throughout my study.

I sincerely thank Dr. Osman G. Ersoy for his invaluable help and academic advice. I would also like to thank all the members of Material Research and Development Center in Arçelik/Tuzla and also Prof. Nihan Nugay, Prof. Turgut Nugay and Cüneyt Bağcıoğlu for their collaboration with this study.

I'll always remember the support of all my friends. There are many names and for the fear of leaving one out accidentally, I will not try.

Last but definitely not least, I thank my family for their unconditional support and encouragement during all my life.

This thesis has been supported by TÜBİTAK Research Project 106T073

ABSTRACT

EFFECTS OF COMPATIBILIZER TYPE AND PROCESSING PARAMETERS ON MECHANICAL PROPERTIES OF POLYPROPYLENE-CLAY NANOCOMPOSITES PREPARED BY MELT MIXING

The effects of compatibilizer type and the processing conditions on polypropylene-clay nanocomposite preparation by melt extrusion were investigated. The objective of the study was to optimize the nanocomposite formulation and manufacturing parameters to obtain enhanced physical and mechanical properties.

The optimum clay content and the compatibilizer type were determined after a series of experiments. Different extruder parameters were used to obtain different shear rate profiles in the extruder. Varying the screw speed and screw design were those parameters. Loading order of the compatibilizing materials was also a parameter that affects dispersion of the clay. The compounds prepared by melt extrusion were injection molded and the specimens were mechanically tested. Then these results were compared to each other.

Considering the test results, the effects of the processing parameters on the physical and mechanical properties of the nanocomposites were discussed.

ÖZET

UYUMLAŞTIRICI TİPİ VE PROSES PARAMETRELERİNİN ERİYİK KARIŞIM YÖNTEMİ İLE HAZIRLANAN POLİPROPİLEN-KİL NANOKOMPOZİTLERİNİN MEKANİK ÖZELLİKLERİNE ETKİSİ

Uyumlaştırıcı tipi ve proses şartlarının, ekstrüzyon yöntemiyle polipropilen-kil nanokompozit eldesine etkileri incelenmiştir. Bu çalışmayla, nanokompozit formülasyonunun ve imalat parametrelerinin optimizasyonu ve böylece gelişmiş fiziksel ve mekanik özelliklere sahip nanokompozitler elde edilmesi amaçlanmıştır.

Kullanılacak kil miktarı ve uyumlaştırıcı tipi, bir dizi deney sonucu saptanmıştır. Ekstrüder içerisinde farklı kesme kuvveti dağılımları oluşturabilmek için farklı ekstrüder parametreleri kullanılmıştır. Bu parametreler, vida dönme hızı ve vida tasarımıdır. Kilin polimer içinde dağılmasına etkiyen bir diğer etmen de uyumlaştırıcıların ekstrüdere yüklenme sırasıdır. Ekstrüde edilen karışımlar, enjeksiyonla kalıplanmış ve kalıplanan bu numuneler mekanik testlere tabi tutulmuşlardır. Elde edilen sonuçlar birbirleriyle mukayese edilmiştir.

Test sonuçları göz önüne alınarak, proses şartlarının nanokompozitlerin fiziksel ve mekanik özelliklerine etkisi incelenmiştir.

TABLE OF CONTENTS

LIST OF FIGURES

LIST OF TABLES

LIST OF SYMBOLS / ABBREVIATIONS

A°	Angstrom
cm	Centimeter
D	Diameter
J	Joule
kg	Kilogram
kN	Kilonewton
kV	Kilovolt
kW	Kilowatt
kWh	Kilowatt hour
L	Length
mA	Miliamper
min	Minute
mm	Milimeter
MPa	Megapascal
M_w	Molecular weight
nm	Nanometer
sec	Second
t	Thickness
w	Width
wt%	Weight percent

λ	Wavelength
Θ	Incident angle

ABS	Acrylonitrile butadiene styrene
BC	Back conveying
FC	Forward conveying
HDPE	High density polyethylene

HDT	Heat distortion temperature
HS	High shear
KB	Kneading block
LDPE	Low density polyethylene
MA	Maleic anhydride
MMT	Montmorillonite
MS	Medium shear
OMMT	Organo- Montmorillonite
PE	Polyethylene
PP	Polypropylene
PP-g-MA	Maleic anhydride grafted polypropylene
PVC	Polyvinyl chloride
rpm	Revolution per minute
SEBS-g-MA	Maleic anhydride grafted styrene-ethylene-butylene-styrene
SME	Specific Mechanical Energy
TEM	Transmission Electron Microscope
TGA	Thermogravimetric Analysis
THF	Tetrahydrofuran
WAXD	Wide-angle X-ray diffraction
XRD	X-Ray diffraction

1. INTRODUCTION

Polymers, reinforced by fibers or other inorganic materials are called polymer composites and they have been commonly used for a long time in industry. However, the term "nanocomposite" just became widespread in early 1990s. The latest technological developments in material science enabled the observation of the morphology of materials at nanoscale; but despite this advance in technology, it is still difficult to prepare compounds at nanometer level.

In this section, a literature review on nanocomposite preparation is presented as categorized in three main titles: the materials used and properties of these materials, manufacturing techniques and characterization of the final nanocomposite.

1.1. Polymer-Clay Nanocomposites

Polymer composites are widely used in science and technology with applications in transportation, construction, electronics, and consumer products. Composites are materials made from two or more constituent materials having different physical and chemical properties. These constituent materials are expected to produce a new material having synergistic properties that those components can not have individually. Constituent materials are categorized in two groups: Matrix and Reinforcement. Commercially, polymers are mostly used as the matrix material and the reinforcement materials are often fibers but also commonly ground minerals.

Composites with having at least one dimension of the dispersed particles in nanometer range (10^{-9} meter) are defined as "nanocomposites". Nanocomposites are a new class of materials showing better physical, thermal and mechanical properties than neat polymer and conventional mineral filled micro or macro composites because of the much stronger interfacial forces between the nanometer-sized domains.

Polymer-clay nanocomposites became widely studied in academic and industrial laboratories with Toyota's work on the exfoliation of clay in nylon-6 in the early 1990s [1, 2]. This revolutionary work demonstrated a significant improvement in mechanical properties by reinforcing polymers with clay on the nanometer scale.

Thermoplastic polymer types used in nanocomposite preparation with layered silicate can be classified as: Vinyls (such as polyvinyl chloride (PVC)), Styrenes (such as acrylonitrile butadiene styrene (ABS)), polyesters, polyamides (such as nylons), polyolefins (such as polypropylene (PP) and polyethylene (PE)) and other special types of polymers [3]. Nanocomposites are commonly based on polymer matrices reinforced by nanofillers. Smectite-type clays, such as hectorite, montmorillonite and synthetic mica, are used as fillers to enhance the properties of polymers. These types of clays have a layered structure. The layers have a high aspect ratio (largest dimension divided by smallest dimension) and each one is approximately 1 nm thick, while the diameter may vary from 30 nm to several microns or larger. Hundreds or thousands of these layers are stacked together with weak van der Waals forces to form a clay particle [4]. Smectite type clays can be modified due to their ion exchange property and this makes them more popular in nanocomposite formation technology.

The main principle in manufacturing polymer-clay nanocomposites is to separate the stacked layer structure of clay aggregates and then separate individual silicate layers in a polymer. By this separation, the number of reinforcing components increases dramatically since each clay particle contains hundreds or thousands of layers and the engineering properties of these individual clay layers will function more effectively. As a result, mechanical properties of the neat polymer will be significantly improved with very low filler loading (typically 5wt% or less) [4].

1.1.1. Forms of Polymer-Clay Nanocomposites

From the nanostructural point of view, two types of polymer-clay nanocomposites are possible: Intercalated and exfoliated nanocomposites. The former is obtained when polymer is regularly inserted into the clay layer galleries and increases the gallery spacing.

Exfoliated nanocomposites are formed when the clay layers are individually dispersed in the polymer matrix [5] (see Figure 1.1).

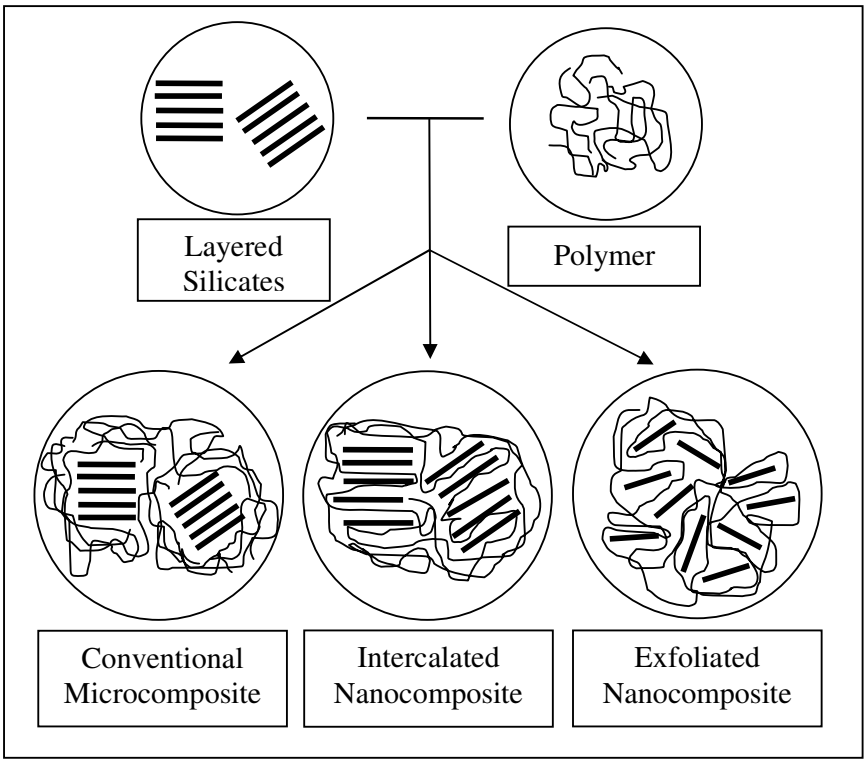

Figure 1.1. Types of polymer-clay composites according to the interaction between layered silicates and polymer.

Intercalated nanocomposites are formed when a small amount of polymer moves into the interlayer spacing between the clay platelets but causes maximum 2 or 3 nanometers separation between them. Exfoliation occurs when polymer further separates the clay platelets by 8 or 10 nanometers or more [6]. This separation may be either uniform or disordered. The silicate layers are individually dispersed in the polymer matrix and each nanolayer contributes to high interfacial interaction with the matrix. This delamination is the main effect that increases the reinforcement property of the nanoclay in the nanocomposite [7].

1.1.2. Polypropylene-Clay Nanocomposites

Soon after the development of nylon/clay nanocomposites achieved by Toyota group [1,2], using clay as a reinforcement material for polymers became a wide area of interest for researchers [7,8].

Nanocomposites can be prepared from a variety of polymers including polyamide, polyethylene, polystyrene, epoxy, polyurethane, etc. but there has been very much interest in polypropylene nanocomposite because of the low cost, low density, high thermal stability and resistance to corrosion properties of PP matrix itself [9]. Due to these good mechanical properties and easy processability, PP can be processed over a wide range of temperatures by various processing techniques [10]. This makes polypropylene to have probably the best price/performance characteristic among all thermoplastics [11].

1.1.3. Polypropylene

Polypropylene which has a chemical formula as $(C_3H_6)_x$ (see Figure 1.2) is a thermoplastic polymer used in a wide variety of applications including packaging, plastic parts, laboratory equipment, automotive components etc. Crystallinity property and Young's Modulus of polypropylene is between that of low density polyethylene (LDPE) and high density polyethylene (HDPE). It is less tough but also less brittle than HDPE, this allows polypropylene to be used as an engineering plastic. Resistance to fatigue, high melting point (130-168 ˚C) and relatively low cost are the other superior properties of PP.

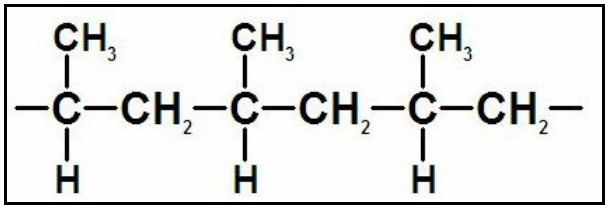

Figure 1.2. Molecular structure of polypropylene chain.

Due to its non-polar nature, PP has high resistance to most solvents and chemicals and also good resistance to moisture. Non-polar structure also makes PP hydrophobic and

makes polar clay minerals and layers difficult to disperse in it. Its highly crystalline nature provides high tensile strength, stiffness and surface hardness to PP.

1.1.4. Layered Silicates

1.1.4.1. Morphology. The commonly used layered silicates in nanocomposite preparation belong to 2:1 phyllosilicates. The word phyllosilicate is originated from the Greek word *phyllon* that means leaf. 2:1 designates that their crystal structure consists of 2 tetrahedral sheets sandwiching a central octahedral sheet. The layer thickness is around 1 nanometer (nm) and the lateral dimension of these layers varies from 30 nm to several microns or larger. These layers are stacked together with a regular van der Waals gap and the spacing in between them is called interlayer or gallery [12].

Montmorillonite is a type of layered silicate which is the most widely used clay as nanofiller. It was first discovered in 1847, in Montmorillon, France but is now found in many locations worldwide. The reason why Montmorillonite (MMT) has received a great deal of attention as a reinforcing filler for polymers is that it has a unique intercalation/exfoliation characteristic, high surface area with a high aspect ratio [13]. The structure of MMT is given in Figure 1.3.

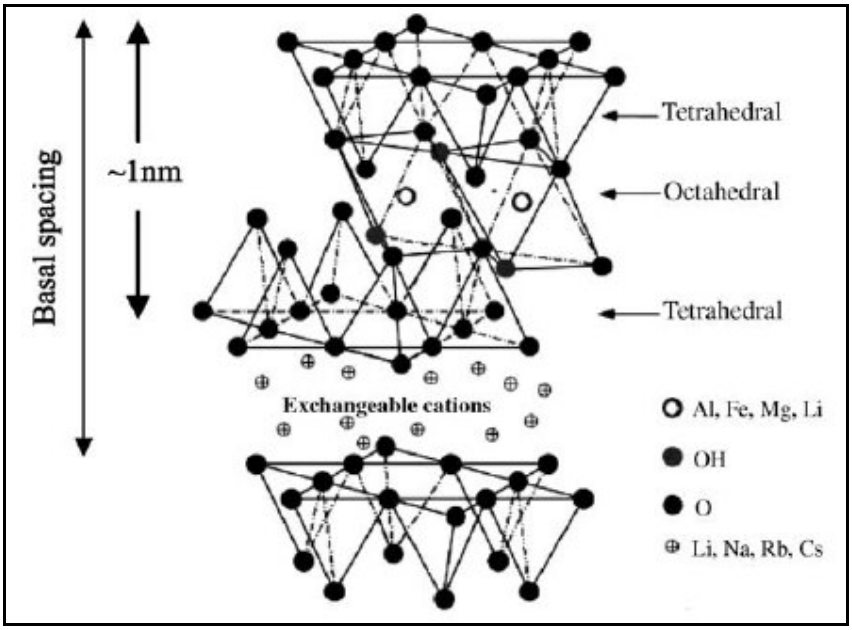

Figure 1.3. The molecular structure of MMT [4].

Layered silicates are expected to have two particular characteristics: The ability of silicate agglomerates to disperse into individual layers and the ability to improve the surface interaction by ion exchange reactions with organic and inorganic cations [4].

1.1.4.2. Modification. Despite its layered structure and high aspect ratio, MMT still does not have a good interaction with most organic polymers since it is hydrophilic. Some chemical modifications have to be applied on MMT to render its surface more hydrophobic and to make it compatible with the polymer.

The clay interlayers are occupied by alkali metal or hydrated cations (Na^{+}). This is caused by the isomorphic substitution (for example, Al^{+3} replaced by Mg^{+2} or Fe^{+2}, or Mg^{+2} replaced by Li^{+1}) within those layers. These cations balance the charge deficiency [4, 14]. Exchanging the cations (Na^{+}) with an organic cation group such as alkyl ammonium is called cation-exchange and these organic modifiers are called intercalants [15]. The incorporation of these organic surfactants into layered silicates expands the interlayers considerably and makes the platelets more compatible with polymers [16].

1.1.5. Compatibilizing Agents

Dispersing clay in a polymer is like trying to disperse oil in water without using detergent. Compatibilizing agents act here as detergent. They are necessary to disperse clay in polymer [17].

It is difficult to mix resin and clay because of the polarity difference between them. Therefore, both polymer and clay have to be modified. Clays are modified with cationic surfactants like organic ammonium salts and they become “organoclays” [18]. For polymers containing polar functional groups, an alkylammonium surfactant is adequate to obtain a nanocomposite formation. However, if polypropylene is used as the polymer, it is necessary to use a compatibilizer.

Polypropylene is the most widely used polymer in polymer-clay nanocomposites. As well as its superior mechanical properties and low cost, polypropylene has also some disadvantages. It is difficult to disperse silicate layers at nanometer level in the matrix and

to obtain an exfoliated structure since PP has a low polarity. The polar groups of the clay silicate layers are compatible only with polymers containing polar functional groups [19].

The homogeneous dispersion of silicate layers was not obtained even by using organophilically modified clay i.e. Organo-MMT (OMMT) because of the lack of polar groups in PP's backbone. Usuki et al. [20] reported a novel approach on preparing a PP nanocomposite by using a functional oligomer (PP-OH) with polar telechelic OH groups as the compatibilizer. Kawasumi et al. investigated the preparation of PP nanocomposites by using a functional polyolefin oligomer (e.g. maleic anhydride grafted PP oligomer) as a compatibilizer [21]. In both case, the interaction between filler and polymer is enhanced by strong hydrogen bonds between the oxygen groups of the silicate layers and the functionalized polymer [11].

Maleic anhydride grafted polypropylene, abbreviated as PP-g-MA, is frequently used in polypropylene nanocomposites since it is miscible with PP matrix and includes a certain amount of polar functional groups. Very promising results have been obtained by using PP-g-MA as a compatibilizer so far. However, due to the chain scission during grafting, PP-g-MA has lower mechanical properties compared with neat polypropylene and this lowers the mechanical properties of the final nanocomposite [22]. Hence, it is crucial to optimize the maleated polypropylene (PP-g-MA) content. High loading of that will have detrimental effects on mechanical properties of the composition where low loading level will not be sufficient for the desirable degree of PP-clay interaction [23].

There are two properties that influence the effectiveness of maleated polypropylene (PP-g-MA) as a compatibilizer: molecular weight and maleic anhydride (MA) content. Several studies about the effects of PP-g-MA on the clay dispersion via melt mixing have been reported so far. As a consequence, despite some inconsistent results, it can be said that, high MA content generally enhances a good intercalation of PP oligomers into clay layers but lowers the mechanical properties of the composite and low molecular weight (M_w) PP oligomers enhance the dispersion of oligomers into clay, whereas high molecular weight oligomers lead to a better improvement in mechanical properties of the composite [24]. Another type of compatibilizer, maleated styrene-ethylene-butylene-styrene (SEBS-g-MA) is used in nanocomposite preparation by Tjong and co-workers [14, 25] and it is

reported that SEBS-g-MA addition improves the tensile ductility, hence impact strength of the nanocomposite.

1.2. Manufacturing Processes of Polymer Nanocomposites

1.2.1. Synthesis of Polymer Nanocomposites

1.2.1.1. In-Situ Polymerization. In-situ is a Latin phrase meaning *in the place* and in chemistry it is used as "in the reaction mixture". In-situ polymerization is the first method used to synthesis polymer-clay nanocomposites. In this technique, the layered silicates of the organoclay are swollen within the liquid monomer or in a monomer solution [12]. Swelling process takes a certain amount of time depending on the temperature and the surface modification of the organoclay. Then, the polymerization is initiated with the addition of a curing agent (for thermosets) or by increasing the temperature (for thermoplastics) as shown in Figure 1.4 [17].

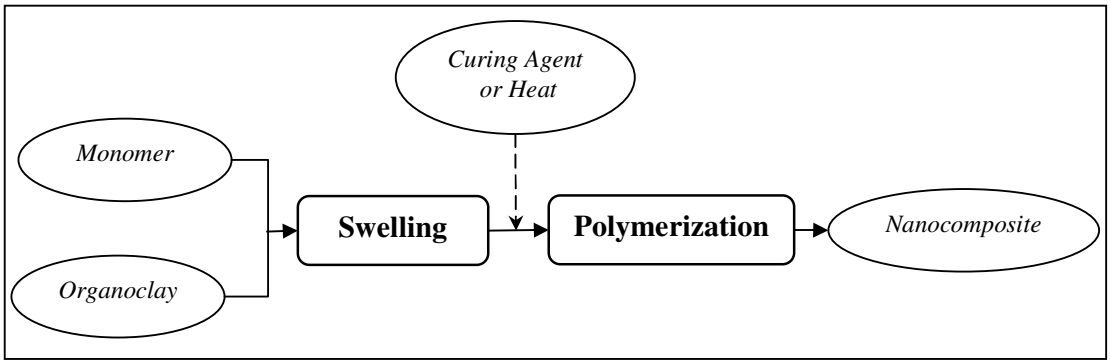

Figure 1. 4. Flowchart of in-situ polymerization.

During the swelling process, polar monomer molecules are attracted by the clay surface energy and then they diffuse between silicate layers so the polymer formation can occur in between these intercalated galleries.

1.2.1.2. Solution. Polymer-clay nanocomposites can also be synthesized by using a polar solvent which is a method similar with in-situ polymerization. Layered silicates have weak forces that stack the layers together so they can be easily dispersed in an adequate solvent. In this method, a polar solvent, such as tetrahydrofuran (THF) or toluene, is used to swell

the organoclay. Then the polymer, dissolved in the solvent, is added to the swollen clay and intercalates between the delaminated clay layers. Finally, the solvent is evaporated and the formation required is provided (see Figure 1.5)

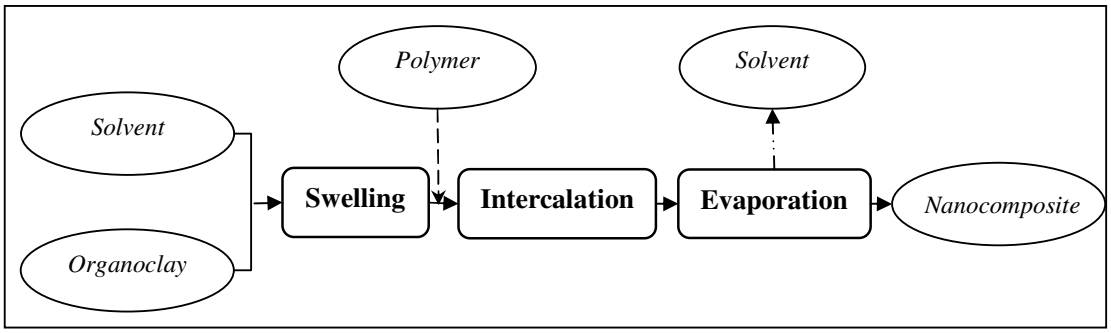

Figure 1. 5. Flowchart of solution method.

It is advantageous to use the solution method because with this technique, non-polar polymers can also be used in synthesis of nanocomposites. However in industrial scale, solution approach can not be applied due to the problems in using large quantities of solvents.

1.2.1.3. Melt Intercalation. The melt intercalation process which was first reported by Vaia et al. [26] is basically blending an organoclay with a molten thermoplastic. After blending process, the mixture is annealed at a temperature above the glass transition temperature of the polymer [17] to form a nanocomposite (see Figure 1.6).

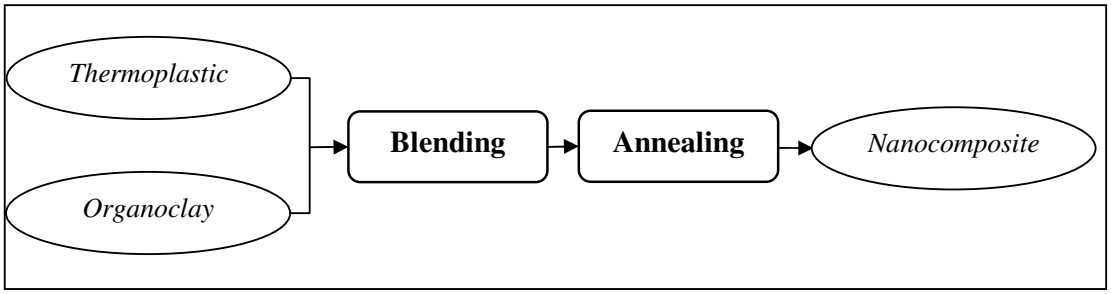

Figure 1. 6. Flowchart of melt intercalation method.

Among the various methods of polymer-clay intercalation, melt intercalation process seems to be the most popular one through its several advantages. This technique is a promising approach for forming nanocomposites since it is significantly more economical

and simple [13] than the other methods. It is also an environmentally benign technique due to the absence of solvents [27]. Although a better exfoliation can be achieved by in-situ polymerization, melt intercalation is more attractive because of commercial feasibility as well as lower cost [28]. Therefore, it has a great potential for application in industry.

Melt delamination of organoclay mechanisms are shown in Figure 1.7. Stacks of clay platelets slide apart from each other and decrease in height. High shear intensity is needed to shear apart these particles (see Figure 1.7b). Polymer chains transport into the silicate layers and push the end of the platelets apart (see Figure 1.7c). This process does not require high shear but involves the diffusion of polymer into the clay galleries by the affinity of polymer with the organoclay surface [6]. Those mechanisms are not separate cases, they can be effective simultaneously.

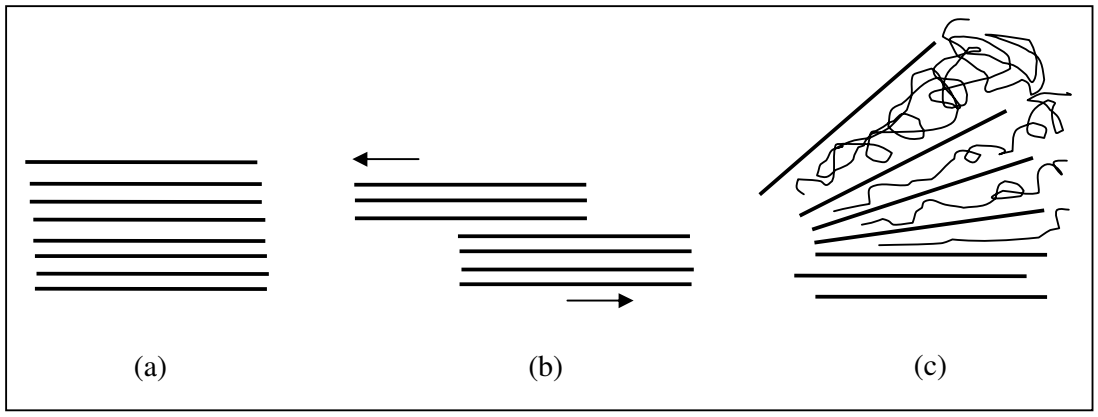

Figure 1. 7. Formation of clay platelets during melt intercalation. Layers are stacked together in (a), then they shear apart by high shear intensity (b) and finally platelets peel apart by polymer diffusion between the galleries (c).

Melt intercalation method is suitable with current industrial processes and allows nanocomposites to be directly formed by compounding devices such as extruders or other types of mixers [13]. In an extruder, melt mixing is occurred under high shearing stress. The final structure and properties of the nanocomposite depends on the extrusion parameters including melt viscosity, shear rate, temperature and pressure and residence time in the barrels of the extruder etc. [29].

Most nanocomposite experiments are carried out by melt intercalation method due to its advantages such as simplicity and lower cost. Compounding devices used in nanocomposite forming provides numerous parameters to be optimized that makes the melt intercalation method attractive for researchers.

1.2.2. Extrusion and Twin Screw Extruders

Polymer melt intercalation is a promising method due to its high productivity, relatively lower cost and compatibility with current polymer processing techniques such as extrusion and injection molding. During extrusion in the processing device, the clay agglomerates are broken up by the external forces and the diffusion of macromolecules into the clay galleries [16].

The extrusion process is not difficult to visualize. A meat grinder is a best model for screw extrusion which is used for plastic processing. The grinder takes a large lump of meat and reduces its size by the screw, mix it all up and then extrude the result through the die. This is a simple example for extrusion process, but in fact there are several process variables that make it harder to optimize [30].

A typical extrusion line consists of the material feed hopper, the extruder (drive, gearbox and screws), the extrusion die, the haul-off and a pelletizer. The components of the extrusion line are regardless of the extruder type and a typical layout is shown in Figure 1.8.

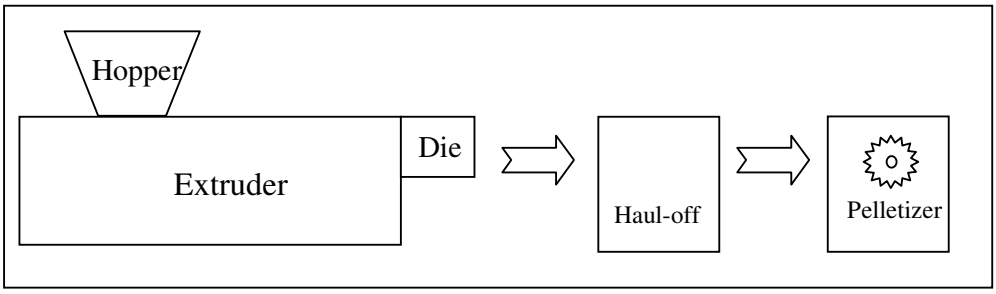

Figure 1. 8. The basic components of an extrusion line.

The hopper holds the raw polymer (in either powder or granule form) and feeds it into the extruder. The extruder has preheated barrels and rotating screw(s) that transports the polymer from feeder to the die exit. Inside the extruder, the molten material is heated, mixed, pressurized and metered simultaneously. At the die the composite takes its final shape and is then cooled while being drawn along by the haul-off device. After cooling (either by water or air), the material is cut by a pelletizer.

The extruder has an electrical motor connected to the screw via a gearbox and drivebelt system. The screw pushes the resin out of the die under high pressure which is balanced with a bearing on the screw. The feed hopper feeds the polymer by a metering screw or a simple conveying spiral. The barrels of the extruder are usually zoned from three to seven sections which are individually heated or cooled to prevent overheating. The molten material moves from the front of the screw to a die channel which forms the shape of the product. Then this product is fed to the saw/cutter that cuts the profile to the desired length.

The extruder screw brings the feedstock into the extruder and moves it along the screw while at the same time compressing it and removing volatile gases. Then heating and mixing of the melt take place. Heating is supplied both from the internally generated shear forces and the additional externally applied heat if required. Finally the melt is metered into the die exit through the pressure applied by the screw. These functions which are shown below in Figure 1.9, take place at different sections in a single screw extruder, whereas simultaneously in a twin screw extruder.

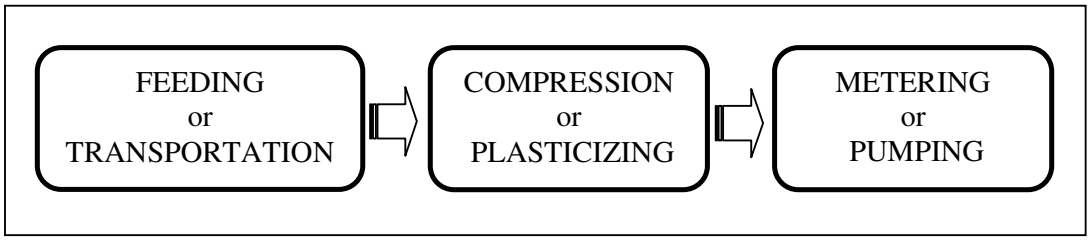

Figure 1. 9. The functions of extruder screw.

Commonly used continuous screw extruders can be classified in two groups: Single screw and twin screw extruders. The former is the most basic form of extruder that simply

melts and forms the material. In contrast, twin screw extruders provide excellent melt mixing and are widely used for polymer nanocomposite manufacturing with different types [30, 31] shown in Figure 1.10.

In addition to this, twin screw extruders are more flexible due to their modular design of screw and barrel and they have better feeding, melting, mixing and degassing properties compared to single screw extruders [31].

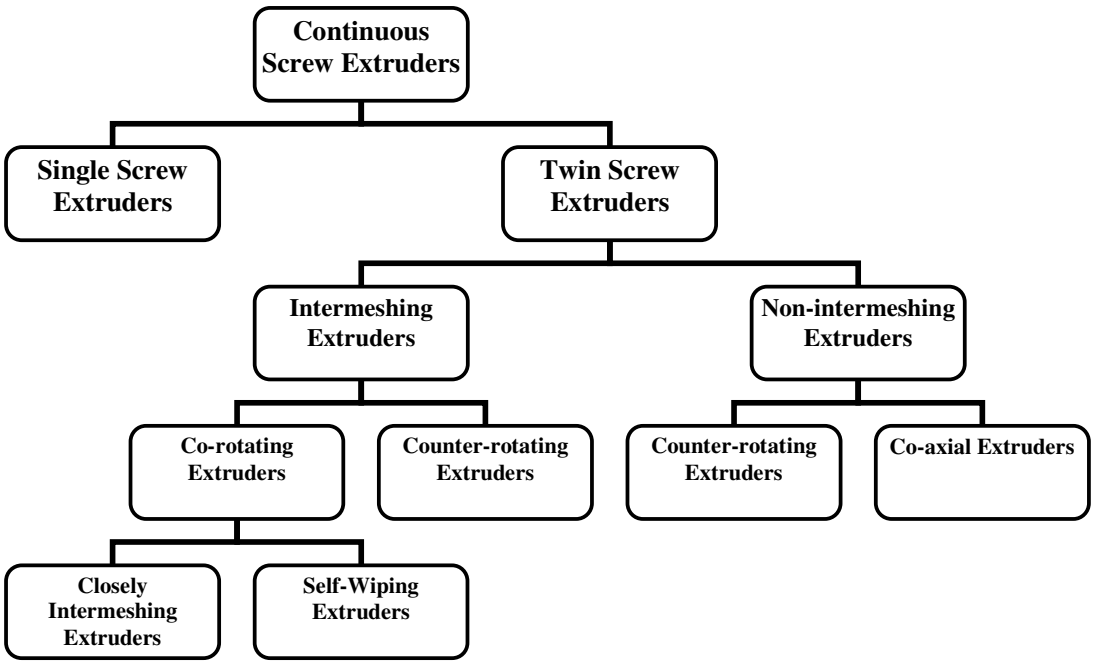

Figure 1. 10. The main types of extruders.

Twin-screw extruders are used extensively in polymer blending and also in many applications such as processing of food, essential oils, paints, and many other highly viscous materials [32,33]. They provide high shear rate and good mixing of compounding materials at a relatively short residence time. In twin-screw extruders, two screws lie adjacent to each other in a barrel casing a “figure-8-pattern” cross section (see Figure 1.11). As illustrated in the diagram above, twin-screw extruders are of many types, such as intermeshing, non-intermeshing, co-rotating, counter-rotating etc. When the screws rotate in the same direction they are called co-rotating but in the opposite direction, then they are known as counter-rotating twin-screw extruders. Twin-screw extruders are named as intermeshing or non-intermeshing depending upon the separation between the axes of their

screws. If the distance between the axes is less than the diameter at the tip of the screw flight, then one screw intermeshes with the other and it is called intermeshing twin-screw extruder. If not it is a non-intermeshing twin-screw extruder. When the flights of one screw wipe the root of the other screw it is a self wiping twin-screw extruder [32]. A drawing of a self-wiping co-rotating intermeshing extruder screws in Figure 1.11 will be explanatory about the screw geometry.

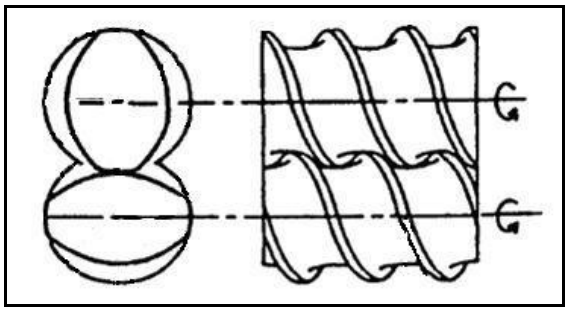

Figure 1. 11. Screw geometry of a self-wiping co-rotating intermeshing extruder.

Twin screw extruders have the superior property that their screw configuration and processing conditions are exchangeable however it is not so easy to control the parameters. The main problem is obtaining the optimum screw configuration and processing conditions in terms of mixing and kneading. When the mixing function of the mixing elements is limited, it can be improved by placing some kneading elements along the screw. These mixing and kneading mechanisms changes various physical properties, such as, flow rate, pressure and shear rate distributions [34]. However, as mentioned before it is hard to measure and control these properties at desired points due to the complicated geometry of screws.

1.2.3. Process Parameters

The state of an extrusion process at any time can be defined by two types of variables. One is called material variables such as temperature, pressure and flow rate and they are related to the material being processed at every point within the device. The other is related to the device itself at every point along its length, hence they are device variables. Barrel temperature profile, screw speed and screw design are some of the device

variables. Measurement and control of the device variables can be applied directly while it is harder to measure and control the material variables [35].

Increasing flow rate, while keeping all other variables constant, results in a less homogeneous product or even in an incompletely melted polymer in the extruder die [36]. Yang et al. [29] have reported the factors that are related to the final structure and properties of composites. They are melt viscosity, shear rate, screw type, barrel temperature and the residence time. Zhu and Xanthos [16] have made a conclusion about extrusion compounding conditions that exfoliation of clay can be obtained by a sufficient long residence time and by a twin screw extruder rather than a single screw one. They also emphasized that excessive shear rate combined with long residence time may break up the exfoliated layers of the nanoclay and lower the aspect ratio of them. Cho and Paul [13] also have called attention to the superior properties of twin screw extruder. They reported that the best delamination of clay can be obtained by an adequate residence time and an appropriate shear rate. Dennis et al. [6] concluded that increasing the residence time and shear rate up to an optimum extent generally improved dispersion of clay. Stacked clay layers shear apart into intercalants by an appropriate shear intensity. According to Lertwimolnun and Vergnes [22], the state of intercalation is unaffected by processing parameters but increasing shear stress, mixing time and decreasing mixing temperature improves clay layer exfoliation. Modesti et al [27] reported that lowering processing temperature increases the shear stress and this condition increases the degree of dispersion. As a consequence about these parameters, it is obvious that preparing the blend at higher shear rates will yield better properties than those prepared at lower shear rates. The better delamination is provided by maximized shear stress conditions such as higher screw speed and lower barrel temperature [10, 27].

Estimated by rheological measurements, Lertwimolnun and Vergnes [37] observed that the intercalated structure of the nanocomposite with an increase in interlayer spacing is unaffected by processing conditions, however, the degree of exfoliation depends on operating conditions such as screw speed and feed rate. Lower feed rate and higher screw speed increase the degree of exfoliation.

Wang et al. [23] has reported that, the feed location and feeding sequences are also very important considerations in dispersing clay platelets. Firstly they fed the base polymer PP upstream at the main hopper and the pre-mixed powder of PP-g-MA and clay downstream at the second barrel. The next trial was feeding the same pre-mixed powder upstream and the base polymer downstream at the fourth barrel. They concluded that the second trial which PP was fed downstream achieved a better dispersion and also gave better mechanical properties.

1.2.4. Screw Design

The proper functioning of the extruder is significantly related to the proper design of the screw geometry. In intermeshing twin-screw extruders, the root diameter of the screws is constant to achieve the self cleaning action; however in single-screw or non-intermeshing twin-screw extruders the root diameter varies along the length [31].

The screw configuration of a twin-screw extruder consists of various mixing elements, such as conveying elements, shearing blocks and kneading blocks. The kneading blocks melt the polymer, disperse the additives in it and mix the melt. Kneading blocks have three types of conveying characteristics: positive displacement (right handed) (see Figure 1.12a), negative displacement (left handed) and neutral (see Figure 1.12b). Negative conveying elements are also called reversely conveying kneading blocks and they provide backmixing during extrusion process. Due to backmixing, reversely conveying kneading blocks configuration offers the largest average residence time compared to other kneading block types. Increase in residence time improves the mixing efficiency. Reversely conveying kneading blocks can also be used to generate local pressure regions. Conveying characteristics of the kneading blocks are obtained by adjusting the staggering angle of the kneading elements [38, 39]. Staggering angles may be various, such as 30˚, 45˚, 90˚. Kneading blocks with different staggering angles have different pumping and kneading capacities. They are chosen and set in order to suit the various processing purposes [40]. If the stagger angle is between zero and ninety degrees, it is a positive displacement (forwarding) kneading block (see Figure 1.12), but if the staggering angle varies from zero to minus ninety, it becomes a reversely conveying kneading block. Neutral kneading blocks have a staggering angle of 90 degrees [31] (see Figure 1.12b).

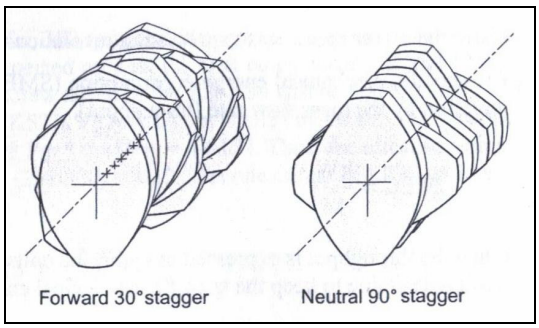

(a) (b)

Figure 1. 12. Forwarding (left) and neutral (right) kneading blocks [31].

Shearer and Tzoganaki [41] reported that the screw configuration with the reverse kneading block exhibited the best mixing due to its larger fully filled volume, where, forward kneading block showed the worst mixing property. The authors also reported that at the low flow rate, forward kneading block exhibited surprisingly good mixing.

According to Rauwendaal's study [42], the best way to visualize the interaction of the screws of a co-rotating twin-screw extruder is to observe the movement of one screw relative to the other. This can be done by rotating screw B around the screw A as shown in Figure 1.13. Both screws are assumed to rotate clockwise and to achieve the correct relative motion between the screws, screw B is not rotating around its own center.

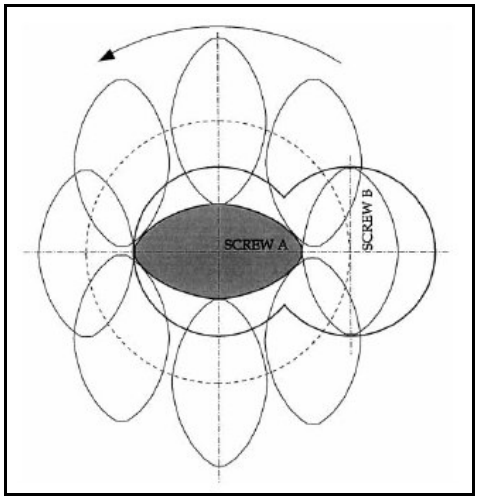

Figure 1. 13. Relative motion of the screws of a co-rotating extruder [42].

1.3. Characterization and Properties of Polymer Nanocomposites

1.3.1. X-Ray Diffraction

X-Ray diffraction is a good method for characterizing the polymer-clay structure by evaluating the spacing between the clay layers. It is one of the diffraction methods and was first conceived by von Laue and the Braggs [43].

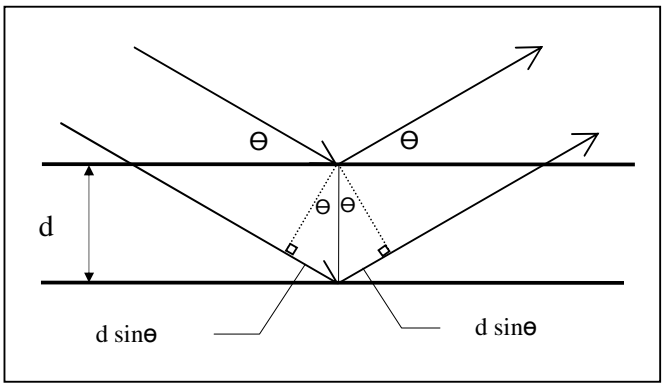

Figure 1. 14. Principle of X-Ray Diffraction

Figure 1.14 shows the diffraction from two parallel planes (silicate layers) having a distance d (basal spacing) between them and intercept X-Rays with an incident angle Θ. The difference in path length for the ray scattered from the top plane and the ray scattered from the bottom plane is $2d*sin\theta$ and according to Bragg's Law, strong diffraction occurs when it is equal to the wavelength λ.

XRD analysis must be sensitive enough to determine the crystalline structure of clay in the nanocomposite, otherwise no peaks appear in the diffraction pattern that may cause a wrong conclusion about dispersion of clay [17, 43].

A sample XRD graph is given in Figure 1.15. Three curves are shown in the graph. The curve at the top belongs to organo-modified MMT (OMMT), it gives a peak, that means its layers are not separated individually although it is modified. The curve in the middle has a little peak and gives information about the structure of an intercalated nanocomposite. Interlayer spacing of the clay was increased but still there are clay

agglomerates in the nanocomposite. The curve at the bottom belongs to an exfoliated structure. Clay layers were dispersed very well and the peak in the curve disappeared.

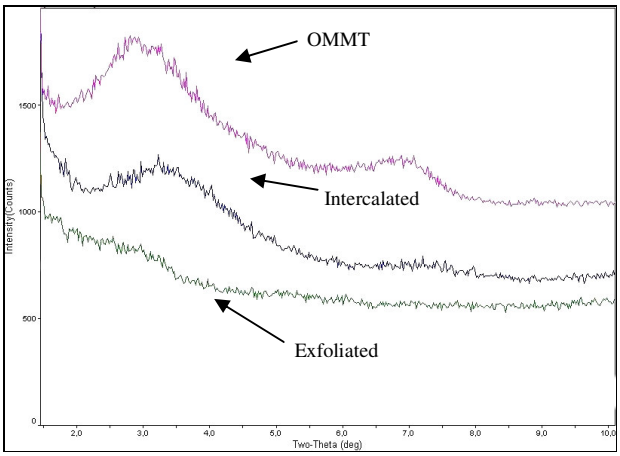

Figure 1. 15. XRD analysis of materials with various structures

1.3.2. Electron Microscopy

Transmission Electron Microscopes (TEM) have become the premier tool for studying structures at nanoscale. Image formation is obtained by the scattering of electrons as the electron beam is transmitted through the sample. TEM allows a precise observation of nanostructure of the nanocomposite and offers a direct image of organoclay tactoids and their delamination in the polymer matrix. Therefore it is employed as a complementary method to XRD analysis. However, time requirement for sample preparation seems to be its disadvantage [17, 43, and 44].

A sample of TEM micrographs was given below. An intercalated zone with unseparated clay layers (see Figure 1.16a) and an exfoliated structure with individual clay layers (see Figure 1.16b) are recognizable.

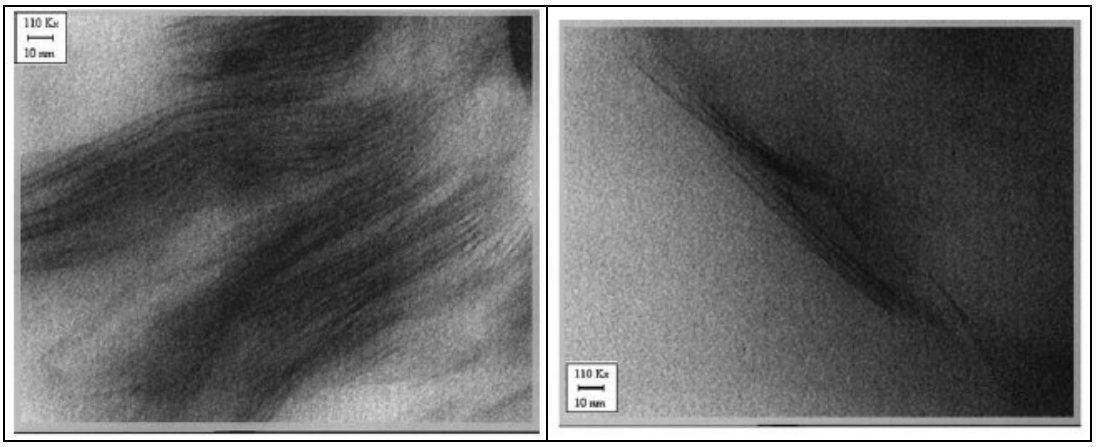

(a) (b)

Figure 1. 16. TEM micrographs of an a) intercalated structure, b) exfoliated structure [27].

1.3.3. Mechanical and Physical Properties

Compared to conventional microcomposites, polymer/layered silicate nanocomposites showed remarkably improved mechanical and physical properties such as increased strength and elastic modulus, increased heat resistance and thermal stability, decreased gas permeability.

Tensile properties of polymer/clay nanocomposites are related to the degree of delamination of silicate layers in polymer matrix, i.e. interaction between the clay layers and the polymer. Tensile modulus (a.k.a. Young's Modulus) expresses the stiffness of the material and it shows a considerable improvement when nanocomposites are formed. It is directly related to the aspect ratio of the dispersed nanolayers and the degree of exfoliation [12]. The general agreement in literature is that, exfoliated nanocomposites show better modulus than intercalated ones. Increasing the clay content results a higher elastic modulus and yield strength up to a critical volume fraction [45]. Breaking stress value of the material strongly depends on the interaction between clay and the polymer; hence, it will be positively affected by the well dispersion of clay. On the other hand, elongation at break value and flexural properties of the nanocomposite are inversely proportional with the clay content that causes brittleness in the material [4]. Fracture toughness of the material also decreases with this brittleness property [17]. Experiments show that the impact properties of the nanocomposite are not affected by clay content [12] but by other additives.

Heat distortion temperature (HDT) of a polymer-based material is an indicator of heat resistance towards applied load. Most of the studies showed that heat distortion temperature increases with clay content and the aspect ratio of the dispersed clay layers [4, 17]. The nano-dispersion of organoclay promotes a higher HDT, while it is difficult to achieve similar enhancement by chemical modification or conventional reinforcement methods [4].

The thermal stability of a polymeric material is observed by Thermogravimetric Analysis (TGA). In this analysis method, degradation at high temperature (a non-oxidative degradation takes place under an inert gas flow) causes a weight loss due to the formation of volatile products. This weight loss is monitored as a function of temperature. It is found that the clay acts as a heat insulator and mass transport barrier to the volatile products and this property of the clay enhances the overall thermal stability of the system. This enhancement can be obtained even at very low filler content [4, 12].

One of the promising properties of polymer/clay nanocomposites is their low flammability that proposes an environmentally benign approach to improve fire resistance of polymers [17]. Gas barrier property of nanocomposites increases with aspect ratio of clay layers. In other words, fully exfoliated structure with long layered silicates will reduce the gas permeability of the nanocomposite [4, 12].

Jordan et al. [45] concluded that the crystallinity of nanocomposites is independent of the size and the filler content. However, the glass transition temperature is increased by increasing clay content. This can be attributable to the retarding effect of the clay layers in the polymer chain.

2. EXPERIMENTAL WORK

All the experimental work (except XRD analysis) of this project was carried out at R&D Material Labs of Arçelik, İstanbul. XRD diffractometer was in Advanced Technologies R&D Center, in Boğaziçi University.

Materials used, manufacturing process and testing procedures of nanocomposites are explained in this section.

2.1. Materials Used

Base polymer matrix used in nanocomposite preparation is polypropylene (PP), grade HE125MO from Borealis, Austria.

Nanofiller which is an organic intercalated nanoclay was supplied from SüdChemie, Germany with its trade mark Nanofil 15.

Two types of compatibilizer are used in this study. Maleic anhydride grafted polypropylene (PP-g-MA) was from ADMER (QF 300E). The other compatibilizer was SEBS-g-MA, with trade mark Kraton FG1901X and with a styrene/rubber ratio 30/70. Both compatibilizers were used to improve the compatibility between the nanofiller and the polypropylene matrix.

2.2. Experimental Procedure

Experiments of this work were done in the following order: Firstly the formulation of the nanocomposite was determined to investigate the effect of the compatibilizer and filler content on mechanical properties of the compound. Then, with this selected formulation, another set of experiments was carried out by varying the process conditions. As a consequence, all these experimental results were compared with each other and the effects of both chemical and mechanical treatments were discussed.

All the experiments and the formulations were given in Table 2.1 in two main groups. Experiments Set # 1 was to determine the compound recipe and the experiments Set # 2 was to examine the effects of process conditions on the mechanical properties of the final nanocomposite.

The first set of experiments was for determining the nanocomposite formulation. Two types of compatibilizers (PP-g-MA and SEBS-g-MA) and three different material contents were tried. The general agreement in literature was that, the mechanical properties of the compound were best when the weight ratio of combatibilizing agent to nanofiller is 3:1. In this work, this proportion was considered as a guide and taken constant and different amounts of nanofiller and compatibilizer were tried; those were 9wt%, 15wt% and 21wt% compatibilizer with 3wt%, 5wt% and 7wt% nanofiller, respectively. In addition to that, an alternative recipe was also tried. PP-g-MA and SEBS-g-MA were used in same formulation with ratio 15wt% and 6wt%, respectively. Here, total compatibilizer ratio of the material was again 21wt%, so the nanofiller ratio was taken 7wt%. PP and the compatibilizer were dry blended and fed from one feeder, where nanofiller was fed from the side feeder.

The next set of experiments was for examining the effects of process conditions on the properties of the nanocomposite. One of the formulations above was selected with respect to the desired mechanical improvements of the nanocomposite and this compound was prepared with different process parameters. Changing the screw speed of the twin screw extruder was the first step. Three different screw speed values were used, 500 rpm which was the standard value for all previous works in this study, 300 rpm and 100 rpm. The screw speed which gave the best result (with respect to the reinforcement of the material) was selected and as a second step, two different screw configurations were tried. One was a high shear (HS) screw which was used for all previous works in this study and the other was a medium shear (MS) screw.

Table 2.1. Formulations and operating conditions of experimental works.

Experiments Set # 1		**Experiments Set # 2**		
Code	Formulation	Code	Formulation	Process Conditions
E1.0	100wt%PP	E2.1	72wt%PP +15wt%PP-g-MA +6wt%SEBS-g-MA +7wt%Nanofiller	HS 500 rpm
E1.1	88wt%PP +9wt%PP-g-MA +3wt%Nanofiller	E2.2	72wt%PP +15wt%PP-g-MA +6wt%SEBS-g-MA +7wt%Nanofiller	HS 300 rpm
E1.2	80wt%PP +15wt%PP-g-MA +5wt%Nanofiller	E2.3	72wt%PP +15wt%PP-g-MA +6wt%SEBS-g-MA +7wt%Nanofiller	HS 100 rpm
E1.3	72wt%PP +21wt%PP-g-MA +7wt%Nanofiller	E2.4	72wt%PP +15wt%PP-g-MA +6wt%SEBS-g-MA +7wt%Nanofiller	MS 100 rpm
E1.4	88wt%PP +9wt%SEBS-g-MA +3wt%Nanofiller	E2.5	76,6wt%PP +15,95wt%PP-g-MA +7,45wt%Nanofiller	PP-g-MA first 100 rpm
E1.5	80wt%PP +15wt%SEBS-g-MA +5wt%Nanofiller	E2.6	72wt%PP +15wt%PP-g-MA +7wt%Nanofiller +6wt%SEBS-g-MA	Added SEBS-g-MA 100 rpm
E1.6	72wt%PP +21wt%SEBS-g-MA +7wt%Nanofiller	E2.7	84,7wt%PP +7,06wt%SEBS-g-MA +8,24wt%Nanofiller	SEBS-g-MA first 100 rpm
E1.7	72wt%PP +15wt%PP-g-MA +6wt%SEBS-g-MA +7wt%Nanofiller	E2.8	72wt%PP +6wt%SEBS-g-MA +7wt%Nanofiller +15wt%PP-g-MA	Added PP-g-MA 100 rpm
E1.8	79wt%PP +15wt%PP-g-MA +6wt%SEBS-g-MA			

The next step for process optimization trials was about loading order of the compatibilizers into the extruder. With the selected screw design and screw speed, four different batches were prepared: PP-g-MA was dry blended with PP and they were compounded with nanofiller in the first batch. This compound was taken from the extruder and dried in a vacuum oven. Afterwards, these granules were dry blended with SEBS-g-MA and fed into the extruder, that was the second batch. SEBS-g-MA was dry blended with PP and compounded with nanofiller for the third batch. This material which was prepared in the third batch was again dried in a vacuum oven and then dry blended with PP-g-MA to be fed into the extruder. This extrusion process was the fourth batch. The nanocomposites had the same formulations at the end of the second and the fourth batch, however, loading order of the compatibilizers were different.

2.3. Manufacturing Process of Nanocomposite

Polymers and fillers were compounded in a twin screw extruder. The final form of the nanocomposite at the die exit looks like spaghettis. After cooling in a water bath, these spaghettis were cut into small pieces by a pelletizer and then these granules were dried in a vacuum oven at 90 ˚C for at least 4 hours. The final manufacturing process was test sample preparation. The nanocomposite granules were taken from the oven and loaded into an injection molding machine. Test specimens to be used in various mechanical tests were produced. Different molds were used for each type of specimens.

2.3.1. Twin-Screw Extruder and Process Parameters

In this work, an intermeshing co-rotating twin-screw extruder was used to manufacture the nanocomposite materials by melt mixing method. The modular twin screw extruder used was PRISM TSE 24 HC (see Figure 2.1), with 24 mm screw diameter (D) and 28:1 L/D ratio (shaft length over screw diameter). Some useful properties according to the producer's (Thermo Electron Corporations) product specifications were given in Table 2.2.

Table 2.2. Technical specifications of Prism TSE 24 HC 28:1 extruder.

PRISM TSE 24 HC 28:1	Units	Values
Barrel bore diameter	mm	24
Screw diameter	mm	23.6
Channel depth	mm	5.15
Max. screw speed	rpm	1000
Power at max. screw speed	kW	9.0
Max. torque/shaft	Nm	43
Barrel zones	Qty.	7
Extruder dimensions L x W x H	cm	165 x 60 x 135

PRISM TSE 24 HC extruder had 7 modular barrel segments, each were heat controlled and had a length of 4D (i.e. 24*4=96 mm). Barrel profiles were illustrated in Figure 2.2. Set temperatures were controlled by electrical resistances and water cooling channels, the 3rd, 5th and 7th barrels had thermocouples mounted to measure the melt temperature of the mixture inside the barrels.

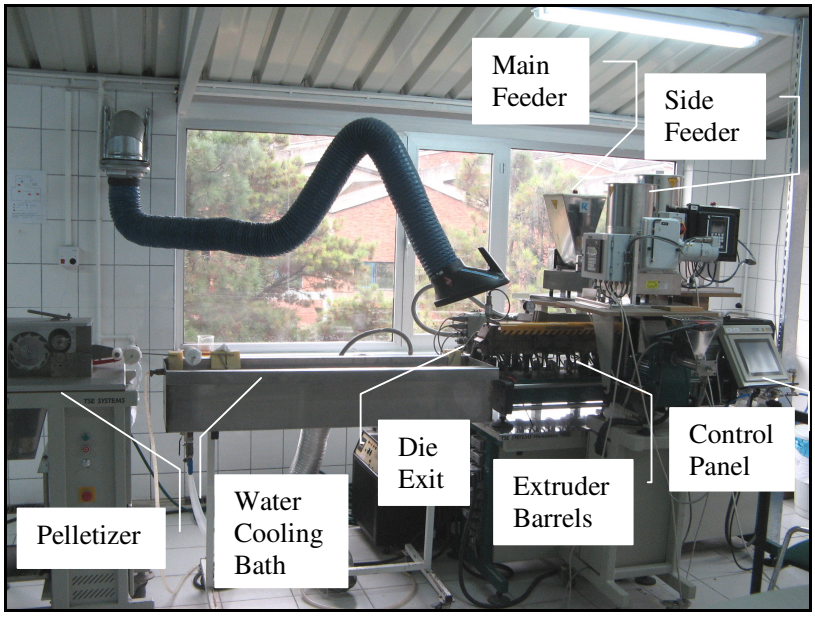

Figure 2.1 PRISM TSE 24 HC modular intermeshing co-rotating twin-screw extruder

The first barrel was called inlet zone, polymeric materials were fed from here and conveyed through the barrels by the effect of torque applied by the extruder screws. At the 6th barrel, there was a degassing unit connected. Gases occurring during the process were removed from here by a vacuum pump. The barrels end with a three-strand hole die and each hole was 3 mm in diameter. The die was mounted at the forward end of extruder, where the molten mixture can go out of the barrels as spaghetti shaped strands. Melt pressure generated by the movement of screws was measured by a pressure sensor connected to the die barrel.

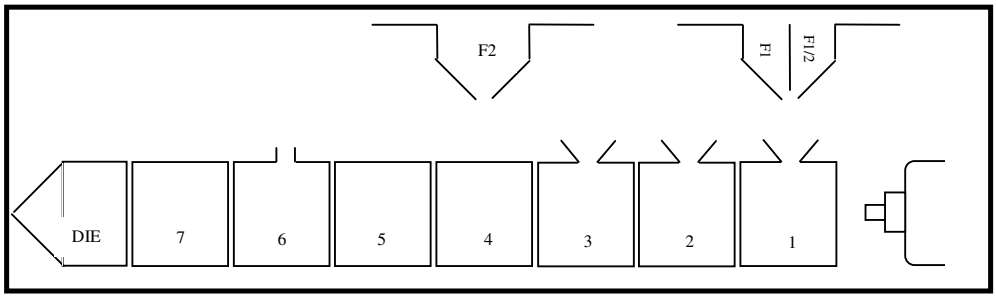

Figure 2.2. Barrel profile

Spaghetti shaped material was cooled down in a water bath (at ambient temperature) and solidified. Then, these spaghettis were cut into small pieces (i.e. granules) by the pelletizer shown in Figure 2.3.

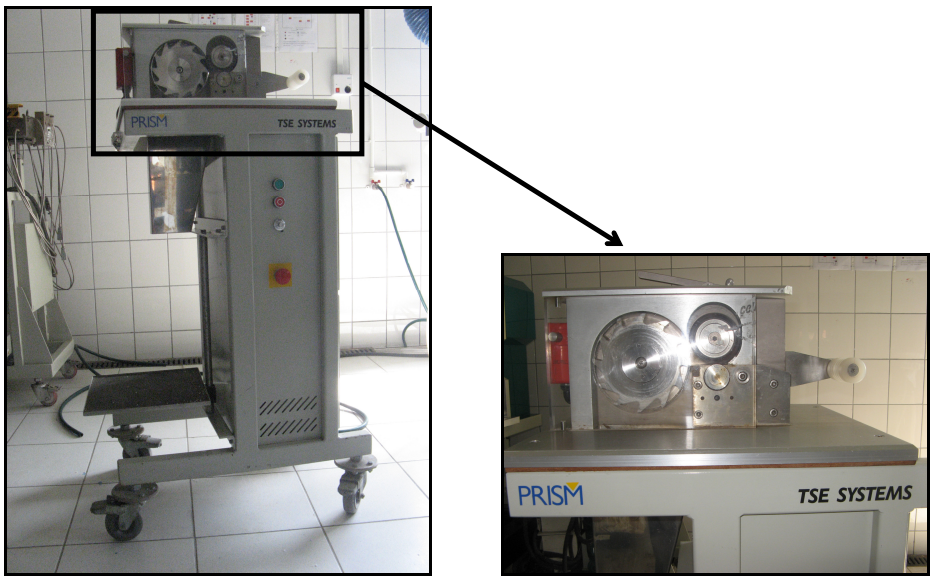

Figure 2.3. Pelletizer

The barrels of the extruder can be split horizontally in the middle for easy screw removal and cleaning purpose as shown in Figure 2.4.

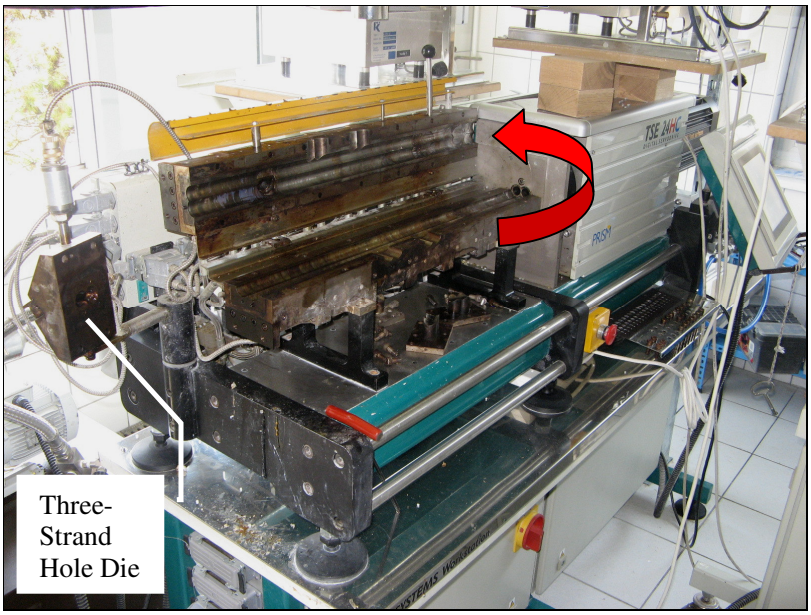

Figure 2.4. Extruder barrel splitted horizontally

The extruder was equipped with 3 feeders. Two of them were K-Tron gravimetric feeders and they were controlled with their own software program. The other was Brabender side feeder and was operated by PRISM controller system.

Experiments set #2 were about comparing nanocomposite materials extruded with different process parameters. First trial was changing the screw speed of the extruder. Experiments in the first set were all done with a screw speed 500 rpm. Here, examining the effects of the screw speed on the mechanical properties of the nanocomposites was aimed so three different screw speed values were tried: 500, 300 and 100 rpm. The screw speed value which gives better results in mechanical tests was selected (here, it is 100 rpm) and by taking this value fixed, the effect of screw configuration was examined.

At this step of the 2nd set of experiments, effects of screw design on mechanical properties of the nanocomposite were investigated with two different screw configurations. One is designed to produce a high shear on the molten material in the extruder and the

other was designed for a medium shear. The high shear (HS) screw had 30˚, 60˚, 90˚ stagger forward and reverse kneading elements and reverse conveying zones. Forward conveying screw elements each had a length D (D=24 mm) and the reverse conveying element used in this screw had a length D/2. The back conveying (BC) and forward conveying (FC) kneading blocks (KB) with staggering angles 30˚, 60˚ and 90˚, and their quantities were shown in Figure 2.5 a.

The medium shear (MS) screw had only kneading elements but no reverse conveying zones. Kneading block of medium shear screw consisted of 5 units of 90˚ stagger elements (neutral), 4 units of 60˚ stagger elements, a wide kneading element and 7 units of 30˚ stagger elements as shown in Figure 2.5 b.

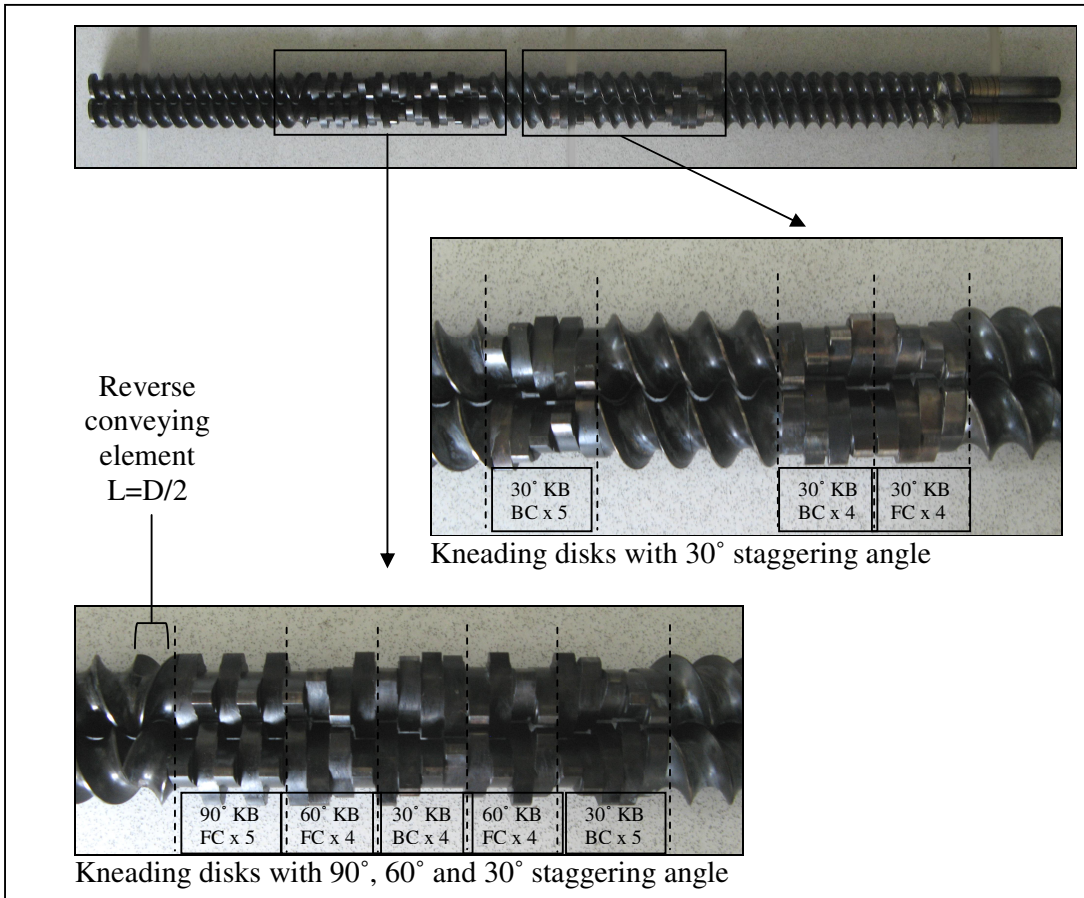

(a) Screw configuration used in high shear screw

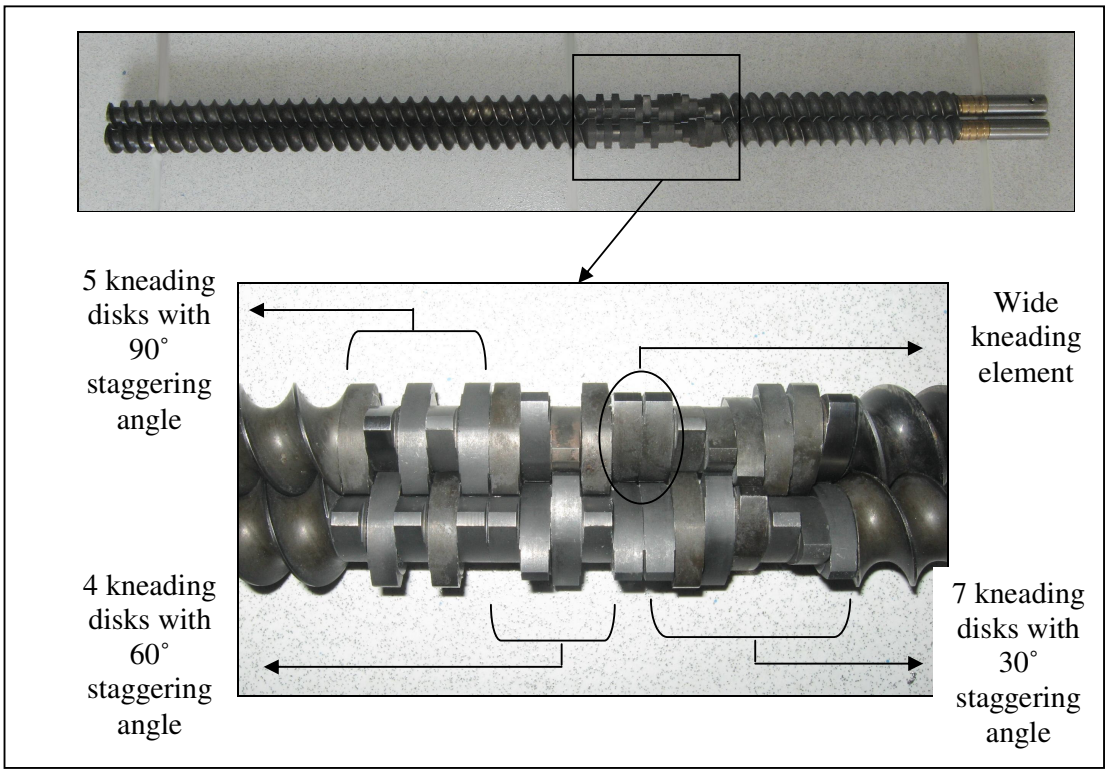

(b) Screw configuration used in high shear screw

Figure 2.5. Screw configurations used, (a) Screw configuration used in high shear screw, (b) Screw configuration used in high shear screw

2.3.2. Injection Molding Machine and Process Parameters

In this work, Arburg Allrounder 320C Injection Molding Machine (Figure 2.6) was used to produce mechanical test specimens: tensile test specimens, and izod impact test specimens. Flexural tests were done by using impact test specimens. Some useful properties according to the producer's (Arburg) product specifications were given below in Table 2.3.

Table 2.3. Arburg Allrounder 320C Injection Molding Machine technical specifications

Arburg Allrounder 320 C	Units	Values
Screw diameter	mm	30
Max. injection pressure	bar	2500
Drive power of the hydraulic pump	kW	15
Max. clamping force	kN	500

Injection molding process is defined as a process where molten plastic is injected at high pressure into a mold cavity. It takes its shape by cooling and solidifying in the mold. Injection Molding Machines consist of 3 main parts: Clamping unit keeps molten material under pressure during injection or cooling; injection unit consists of hopper, cylinder and screw; and finally mold is the part where the material cools down and takes its shape.

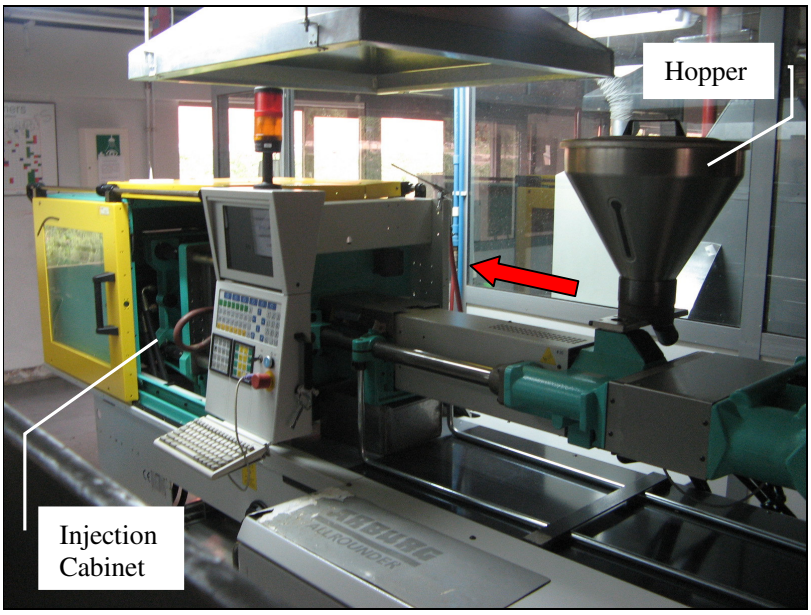

Figure 2.6. Arburg Allrounder 320C Injection Molding Machine

Injection molding machine was fed by granule shaped nanocomposites. These granules were melted by heat through the screw. When the molten material came out the screw, injection began and the material was forced into the mold cavity by the movement of the screw. The screw held the force for a short period to compensate for the shrinkage of the material. After the injection and holding the pressure, the mold was kept closed for cooling down. The material solidified, took its shape and then forced out of the mold by ejectors. Excessive parts of the product, such as runners and gates of the cavity, were cut by a belt saw, Rexon.

While manufacturing the test specimens for examining the mechanical properties of the nanocomposites, three types of molds were used to produce three types of samples. Normal tensile mold for tensile testing; weld-line tensile mold for weld-line tensile testing

and impact mold for both flexural and impact testing (Figure 2.7). The shape and the dimensions of the weld-line tensile test specimen were same as the normal tensile one; however, the former was fed from two points into the cavity, so molten polymeric material met in the middle of the specimen creating a possible failure zone.

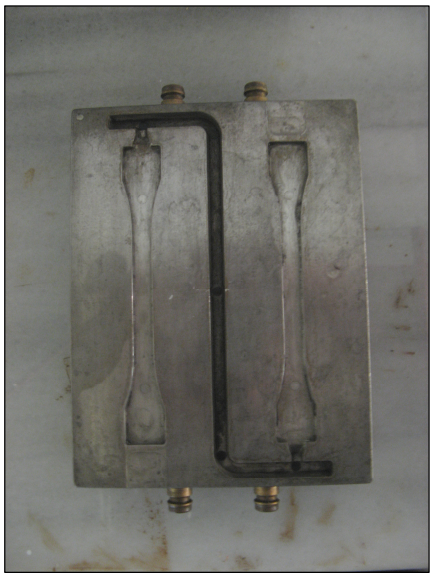

(a) Tensile test specimen (ISO R527)

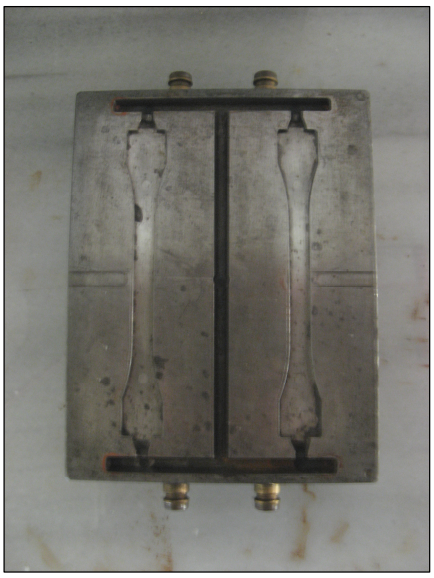

(b) Weld-line tensile test specimen (ISO R527)

(c) Flexural and impact test specimen (ISO 178, ISO180)

Figure 2.7. Molds designed for test specimens, (a) Tensile test specimen (ISO R527), (b) Weld-line tensile test specimen (ISO R527), (c) Flexural and impact test specimen (ISO 178, ISO180)

Time and pressure values of the three steps of injection and holding processes for the test specimens were shown in Table 2.4. Injections parameters were also given below.

Table 2.4. Injection and holding process parameters of Injection Molding Machine

Normal Tensile Test Specimen	**Unit**	**1st Step**	**2nd Step**	**3rd Step**
Injection Speed	cm^3/sec	120	125	110
Injection Pressure	bar	750	800	750
Holding Time	sec	0.2	5	3
Holding Pressure	bar	750	700	500
Shot Volume	cm^3	36		
Screw Speed	rpm	140		
Backpressure	bar	25		
Weld-line Test Specimen	**Unit**	**1st Step**	**2nd Step**	**3rd Step**
Injection Speed	cm^3/sec	120	125	110
Injection Pressure	bar	750	800	750
Holding Time	sec	0.2	5	3
Holding Pressure	bar	750	700	500
Shot Volume	cm^3	41.6		
Screw Speed	rpm	140		
Backpressure	bar	25		
Flexural and Impact Test Specimen	**Unit**	**1st Step**	**2nd Step**	**3rd Step**
Injection Speed	cm^3/sec	110	140	120
Injection Pressure	bar	850	1000	900
Holding Time	sec	0.2	5	3
Holding Pressure	bar	850	800	675
Shot Volume	cm^3	37		
Screw Speed	rpm	140		
Backpressure	bar	25		

2.4. Testing and Characterization of Nanocomposite

Nanocomposite materials which were melt compounded in twin screw extruder were tested for physical and mechanical properties using various procedures.

2.4.1. Physical Properties

Polymer/clay nanocomposites were arranged into two groups according to the interaction between silicate layers and the polymer matrix, as mentioned in Introduction section. To see whether they are intercalated or exfoliated, XRD Analysis was needed. Graphs with a clear peak designate the interlayer distance and they were an evidence for intercalated nanocomposites, whereas graphs with no peak showed signs of exfoliation in the nanocomposite.

Wide-angle X-ray diffraction (XRD or WAXD) measurements were conducted on a Rigaku-D/Max-2200 Ultima Diffractometer (Rigaku, Tokyo, Japan) with CuK_{α} radiation (λ=1,54 Å), operating at 40 kV and 40 mA and a scanning rate of 2º min^{-1}. The scanning range was from 1.5º to 10º. Before the analysis began, nanocomposite materials to be examined in X-Ray Diffractometer were transformed from granules to powder by a chopper.

2.4.2. Mechanical Properties

Injection molded test specimens were brought to an air conditioned room and they were left here for at least 48 hours to eliminate the effects of post crystallization. Room temperature was fixed at 23±2 ˚C and the relative humidity was 50%. The mechanical tests were also performed at these conditions.

Four types of mechanical tests were applied on the nanocomposites. Normal tensile, weld-line tensile, flexural and impact resistance properties were measured in these tests and were reported below.

2.4.2.1. Normal Tensile Test. Tensile strength of the materials was measured by a Zwick Universal Tensile Testing Machine Z020 according to ISO R 527 standard [46]. Load indicator equipment was a 20 kN load cell and extension indicator was a mechanical long stroke extensometer.

Test specimens were left at the air conditioned room (23±2 ˚C and 50% relative humidity) for at least 48 hours, and then measured in thickness and width before testing to obtain the cross section area of the sample (Figure 2.8). Both tensile and weld-line tensile test specimens are 150 mm in length and 3 mm in thickness. Afterwards, the specimen was fixed to self-aligning grips of the tensile test machine with 123 mm distance between grips. The extensometer was attached to the specimen and the gage distance of the extensometer was 700 mm. Test was performed at a constant speed of 50 mm/min and the stress and corresponding strain values were recorded at 0.1 second time intervals.

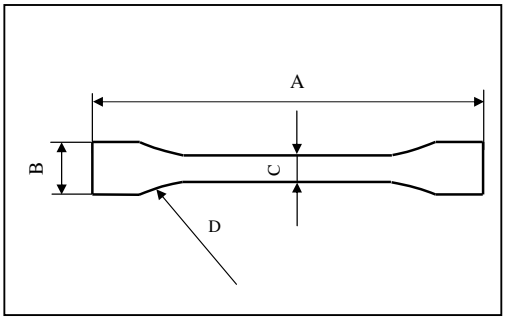

A Overall length, minimum:	150 mm
B Width at ends:	20±0.5 mm
C Width of narrow parallel portion:	10±0.5 mm
D Radius, minimum:	60 mm

Figure 2.8. Tensile test specimen according to ISO R527 [46]

Following tensile properties were reported at the end of the test:

- Maximum stress [N/mm^2]
- Strain at maximum load [%]
- Stress at break [N/mm^2]
- Strain at break [%]
- Elastic Modulus (a.k.a. Young Modulus) [N/mm^2]

- Work up to maximum load [Nmm]

2.4.2.2. Weld-Line Tensile Test. Weld-line tensile properties of the nanocomposite samples were examined by the same Tensile Testing Machine and with the same process settings as the tensile testing.

In weld-line tensile testing, unlike normal tensile testing, only the tensile properties of the weld-line of the specimen were investigated. Hence, only the dimensions of the weld line (width and thickness) were taken account in calculations (Figure 2.8). Properties reported were the same as normal tensile testing:

- Maximum stress [N/mm^2]
- Strain at maximum load [%]
- Stress at break [N/mm^2]
- Strain at break [%]
- Elastic Modulus (a.k.a. Young Modulus) [N/mm^2]
- Work up to maximum load [Nmm]

2.4.2.3. Flexural Test. Flexural properties of the nanocomposite materials were measured by an Instron 4505 Universal Tensile Testing Machine according to ISO 178 [47]. Load indicator equipment was a 10 kN load cell. A three point bending fixture was used for testing.

Izod impact test specimens were used for flexural testing. Considering ISO 178 standards, specimens were 80±0.5 mm in length (L), 10±0.5 mm in width (w) and 4±0.2 mm in thickness (t) as shown in Figure 2.9. All the test specimens were measured by a micrometer with 0.02 mm sensitivity before testing to obtain the cross section area. These specimens were tested after a 48 hours from injection molding. They were left in an air conditioned room for 48 hours at 23±2 ˚C and with 50% relative humidity. Flexural test was also performed at these conditions.

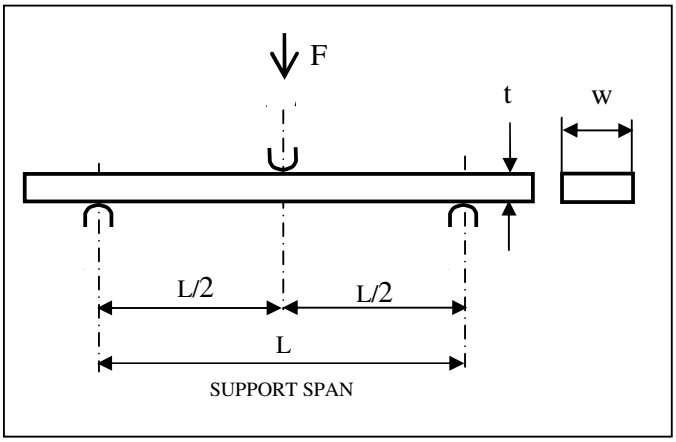

Figure 2.9. Flexural test specimen loaded in three point bending

The specimen was put on the lower arm of the bending fixture connected to the stationary testing machine base. The upper arm of the fixture which was connected to the movable crosshead of the testing machine was slowly contacted with the test specimen at mid-span and the test was started. Test was performed at a constant speed of 5 mm/min and the load and corresponding extension values were measured by travel distance of the movable part and they were recorded in a 0.2 second time interval.

Following flexural properties were reported at the end of the test:

- Stress at yield [N/mm^2]
- Strain at yield [%]
- Elastic Modulus (a.k.a. Young Modulus) [N/mm^2]

2.4.2.4. Impact Test. Izod impact strength of the test materials was measured by a Zwick Impact Tester which tests up to 2.75 Joules by the versatile impact pendulum according to ISO 180 standard [48].

Injection molded test specimens were left for 48 hours to eliminate the effects of post crystallization and then tested in an air conditioned room (with a temperature 23±2 ˚C and with 50% relative humidity). Specimen dimensions were 80±0.5 mm in length, 10±0.5 mm in width and 4±0.2 mm in thickness considering ISO 180 standard. All the test specimens were measured by a micrometer with 0.02 mm sensitivity before testing to obtain the cross section area. Afterwards, 2 mm notch (v-shaped) was machined at mid-span of specimen.

A test without a specimen was done to confirm the frictional loss which is 0.038 J. Then the specimen was placed into the grips of the testing machine and the pendulum was released. The notched surface should be faced to the impact point (see Figure 2.10).

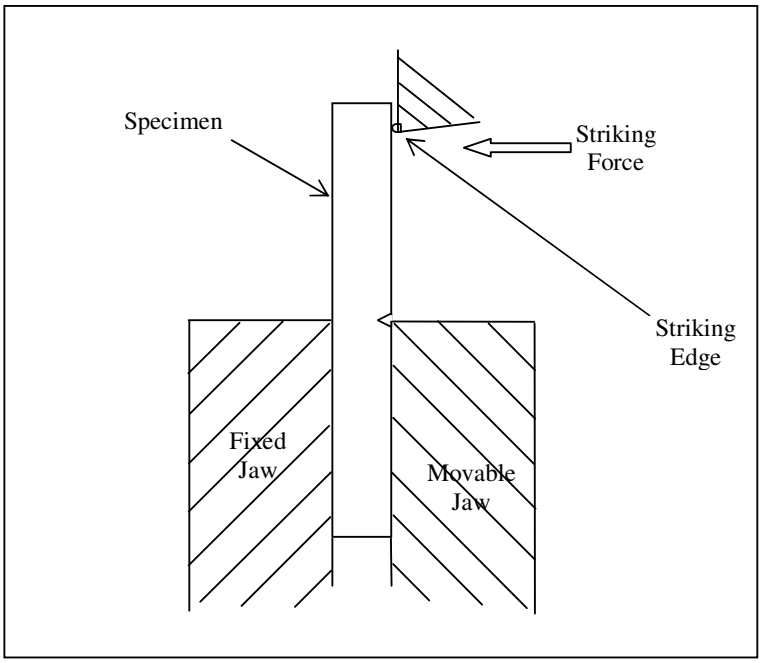

Figure 2.10. Izod Impact test setup

The impact energy was measured and by the addition of frictional loss, the correct impact energy [J] was calculated. The Izod impact strength [kJ/m^2] was calculated by the dividing the impact energy to the cross-section area of the sample.

3. RESULTS AND DISCUSSION

Experimental work of this study was carried out by repeating the tests at least five times (ten for impact test) for each group of specimen. The results obtained were tabulated and compared with each other. They were shown in graphs by trend lines passing through the value points.

3.1. Physical Properties

XRD analysis gave information about the physical properties of the nanocomposites. Degree of dispersion (intercalation/exfoliation) of the clay was determined by this analysis. Table 3.1 below shows the d-spacing values of the nanocomposites if exist. Most of the nanocomposites in this study showed reduced peak shifts that means they were intercalated. Only the nanocomposites with SEBS-g-MA (E1.4, E1.5, and E1.6) were exfoliated but the other compounds exhibited increased basal spacing as compared to the raw organo-modified MMT (For XRD curves of OMMT, E1.3 and E1.6 see Figure 1.15).

Table 3.1. XRD results of the nanocomposites

Code	**Nanocomposite Formulation**	**d-spacing (A˚)**
OMMT	Nanofil 15 (organo-modified MMT)	29.3261
E1.1	88wt%PP+9wt%PP-g-MA+3wt%Nanofiller	29.6403
E1.2	80wt%PP+15wt%PP-g-MA+5wt%Nanofiller	31.4940
E1.3	72%PP+21%PP-g-MA+7%Nanofiller	28.7680
E1.4	88wt%PP+9wt%SEBS-g-MA+3wt%Nanofiller	NO PEAK
E1.5	80wt%PP+15wt%SEBS-g-MA+5wt%Nanofiller	NO PEAK
E1.6	72wt%PP+21wt%SEBS-g-MA+7wt%Nanofiller	NO PEAK
E1.7	72wt%PP+15wt%PP-g-MA+6wt%SEBS-g-MA+7wt%Nanofiller	33.9446
E2.1	72wt%PP+15wt%PP-g-MA+6wt%SEBS-g-MA+7wt%Nanofiller (500 RPM)	32.3475
E2.2	72wt%PP+15wt%PP-g-MA+6wt%SEBS-g-MA+7wt%Nanofiller (300 RPM)	31.6575
E2.3	72wt%PP+15wt%PP-g-MA+6wt%SEBS-g-MA+7wt%Nanofiller (100 RPM)	31.8748
E2.5	76,6wt%PP+15,95wt%PP-g-MA+7,45wt%Nanofiller (100 RPM)	29.6295
E2.6	72wt%PP+15wt%PP-g-MA+7wt%Nanofiller+6wt%SEBS-g-MA (100 RPM)	30.5562
E2.7	84,70wt%PP+7,06wt%SEBS-g-MA+8,24wt%Nanofiller (100 RPM)	33.0666
E2.8	72wt%PP+6wt%SEBS-g-MA+7wt%Nanofiller+15wt%PP-g-MA (100 RPM)	31.1956

3.2. Mechanical Properties

The first set of experiments was for determining the optimum nanocomposite formulation. For this purpose, various clay ratios and compatibilizer types were tried. As the second set, effects of process conditions were examined. These conditions were related to the manufacturing process in the twin screw extruder. Screw speed, screw design and loading order of the materials were the process conditions examined.

A typical stress-strain curve of a tensile testing in this study was given as a sample in Figure 3.1 a. There were five curves belonging to five tests of the same material. Maximum stress value is the peak value of the curve. Strain at maximum force is the percent elongation at maximum force value. Elastic modulus was the slop of the linear portion of the curve (elastic region). Work up to maximum force was obtained by the related area underneath the stress-strain curve. Figure 3.1 b showed a graph of flexural test. All the test values were plotted and then the average value was calculated. Calculations of flexural stress and deflection values were carried out according to ISO178 standard [47].

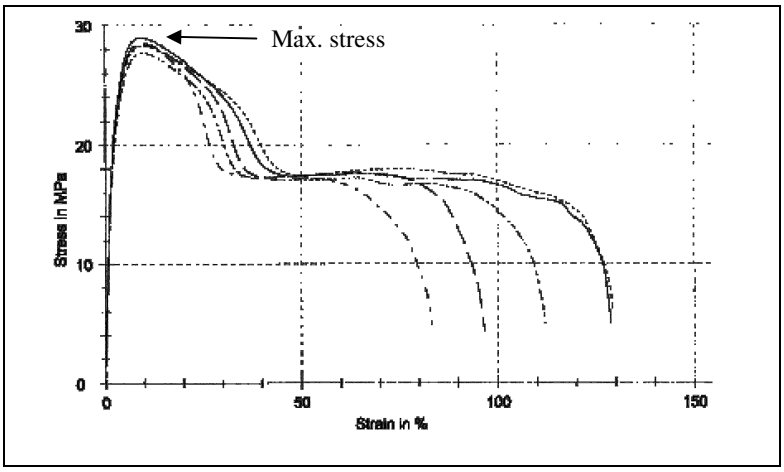

a) Stress-strain curve of tensile testing

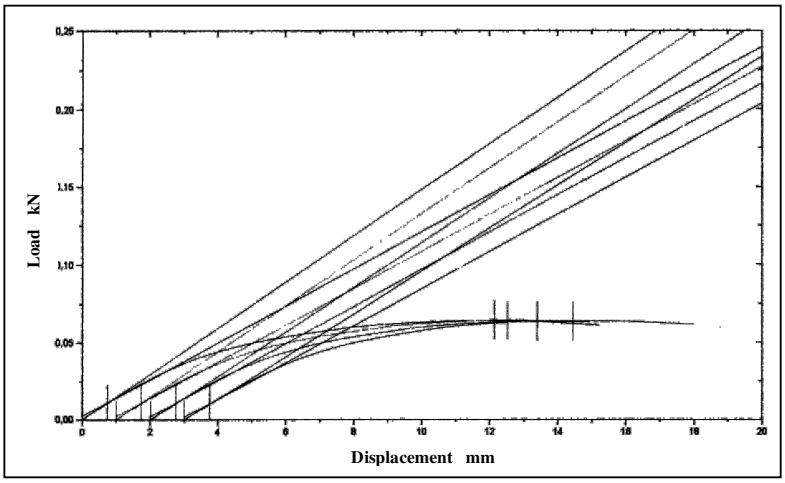

b) Load-displacement curve of flexural testing

Figure 3.1. Typical test curves for tensile and flexural testing, a) Stress-strain curve of tensile testing, b) Load-displacement curve of flexural testing

3.2.1. Nanocomposite Properties with respect to Clay Content

The role of the clay content in the nanocomposite formulation was investigated by using three different ratios: 3wt%, 5wt% and 7wt%. In one set, PP-g-MA was used as compatibilizer with these clay ratios, in the other set experiments were repeated with the same clay contents but with SEBS-g-MA as the compatibilizer. Clay/compatibilizer ratio was kept constant at 1:3 in weight. All the test results were shown in Table 3.2 and plotted separately in Figure 3.2 a to f. To keep the graphs simple, only the normal-tensile values were given remembering that the weld-line tensile values give -more or less- the same trend.

Table 3.2. Nanocomposite mechanical test results with respect to clay content (The standard deviations are given in parenthesis).

	PP	**E1.1**	**E1.2**	**E1.3**	**E1.4**	**E1.5**	**E1.6**
Max Stress [MPa]	33.25 (1.02)	35.47 (0.34)	34.79 (0.12)	34.10 (0.27)	28.28 (0.20)	26.30 (0.10)	23.19 (0.09)
Strain at Fmax [%]	9.05 (0.14)	7.43 (0.27)	7.08 (0.06)	6.92 (0.17)	9.17 (0.15)	9.66 (0.04)	11.46 (0.30)
E Modulus [MPa]	1429.07 (125.98)	1666.84 (56.81)	1691.53 (68.44)	2021.10 (41.24)	1317.78 (65.95)	1182.74 (28.74)	1000.23 (70.96)
Work up to F_{max} [Nmm]	5052.76 (145.93)	4346.46 (84.94)	4086.86 (45.85)	3982.55 (109.24)	4496.18 (71.97)	4424.76 (28.26)	4659.42 (114.15)
Stress at Yield (Flex. Test)[MPa]	38.84 (0.56)	43.59 (0.20)	42.83 (0.22)	42.53 (0.20)	33.32 (0.22)	30.94 (0.19)	29.81 (0.35)
Impact Strength [kJ/m^2]	2.89 (0.16)	3.29 (0.12)	3.16 (0.07)	3.46 (0.24)	4.07 (0.39)	5.46 (0.25)	7.10 (0.59)

Increasing the clay content from 3wt% to 7wt% in experiments with PP-g-MA (batches E1.1, E1.2, E1.3 of Table 2.1), only slight improvement in strength (Figure 3.2a and e) and impact properties (Figure 3.2f) was observed but a good enhancement in elastic modulus (Figure 3.2c) was noted. However, strain at maximum force and work up to maximum force were slightly decreasing while clay ratio was increasing as shown in Figure 3.2b and d indicating that ductility of the nanocomposite is reducing with increasing clay content. Nanocomposites with 7wt% clay content became more brittle but not tough enough. This might be caused by poor dispersion of the filler and poor compatibilization between the clay and the polymer matrix.

These tensile strength results nearly converged to the values given in the study of Garcia-Lopez et al. [19] for PP-g-MA compatibilized nonocomposites. They used two different OMMT types. Either when the OMMT/PP-g-MA ratio was 3/9 [wt%] or 7/21 [wt%], their tensile strength values were within ±1 MPa range when compared to E1.1 and E1.3 in this study. The elastic modulus results they obtained were 20-28 % better than those obtained in this study. This might have been due to the clay type or processing conditions. The batch with 21wt% SEBS-g-MA (E1.6) gave a much better elastic modulus result but slightly lower tensile strength values when compared to the study of Tjong and Meng [25] where 20wt% SEBS-g-MA is used with a different type of modified silicate clay.

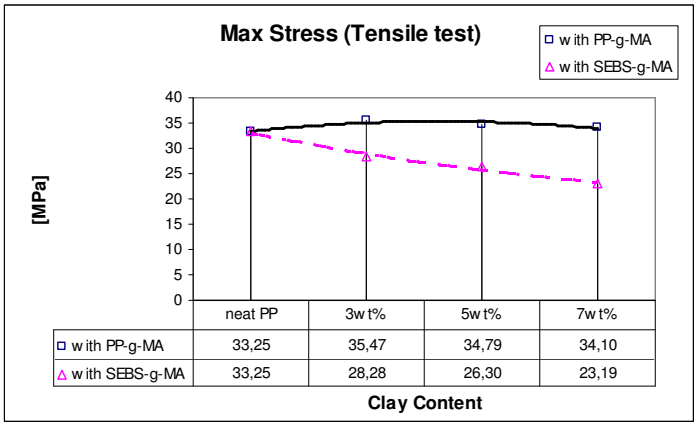

(a) Maximum stress values of tensile testing

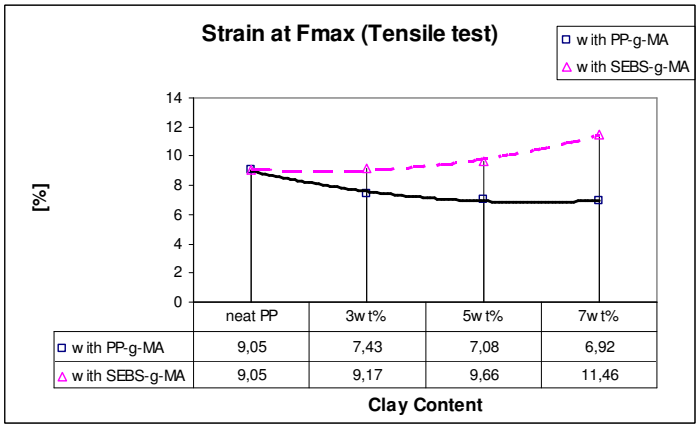

(b) Strain at maximum force values of tensile testing

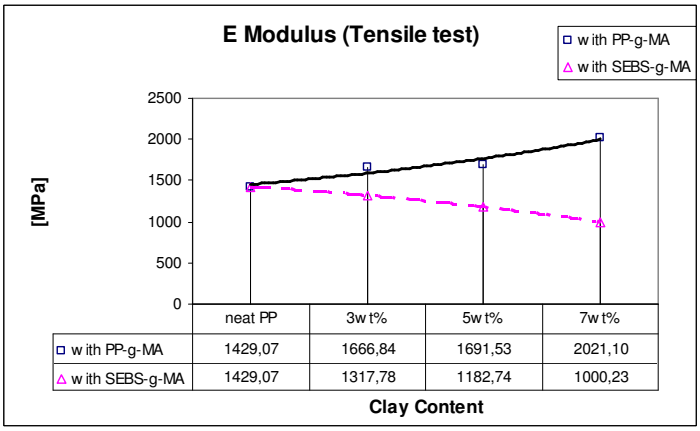

(c) Elastic modulus values of tensile testing

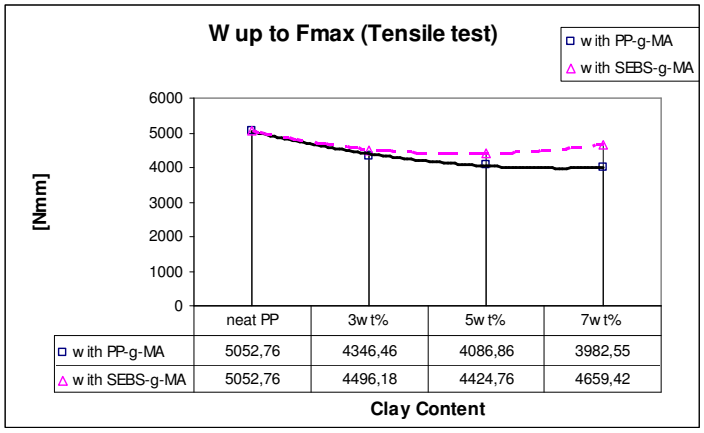

(d) Work up to maximum force values of tensile testing

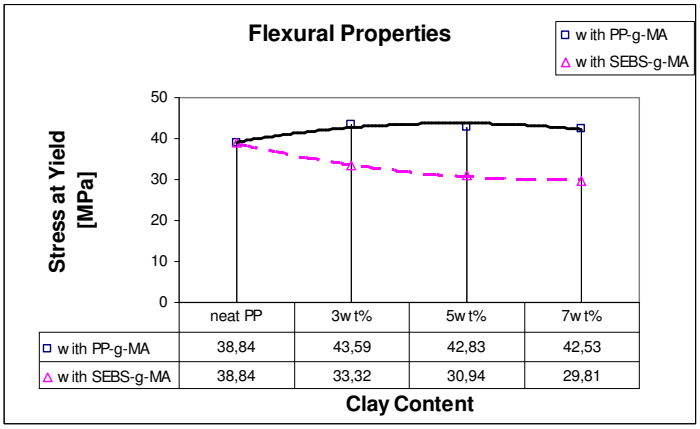

(e) Flexural test (Stress at yield values)

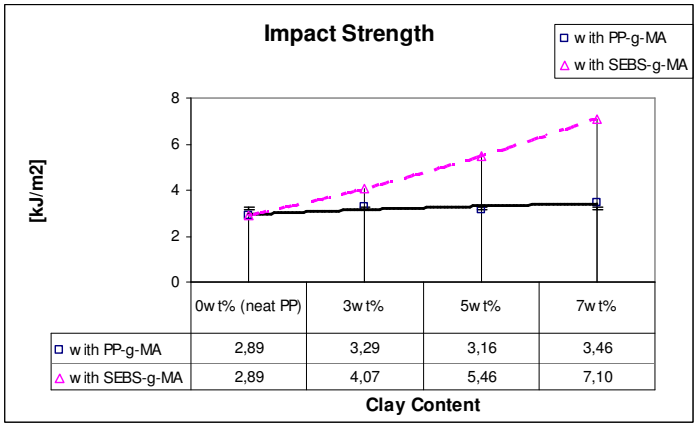

(f) Izod-impact test values

Figure 3.2. Nanocomposite mechanical test results with respect to clay content, (a) Maximum stress values of tensile testing, (b) Strain at maximum force values of tensile testing, (c) Elastic modulus values of tensile testing, (d) Work up to maximum force values of tensile testing, (e) Flexural test (Stress at yield values), (f) Izod-impact test values

Batches E1.4, E1.5, and E1.6 were prepared with clay contents of 3wt%, 5wt%, 7wt% and SEBS-g-MA contents of 9wt%, 15wt%, 21wt%, respectively (see Table 2.1). Strength properties and elastic modulus were decreasing with increasing clay ratio (see Figure 3.2a, c and f). In contrast, strain at maximum force was increasing by clay ratio since SEBS-g-MA which contains rubber was also increasing with the clay ratio (see Figure 3.2b, d and f). The impact strength of the material was dramatically increased by the clay content. Hence the clay content of 7wt% became advantageous by this hopeful development. But here, the increase in impact strength is most likely to be attributable to increase in rubber (SEBS) content since the impact strength of PP-g-MA compatibilized nanocomposites were not increasing this much with clay content.

3.2.2. Nanocomposite Properties with respect to Compatibilizer Type

Compatibilizers were auxiliary materials providing better interaction between the nanoclay and the polymer matrix. In this study PP-g-MA and SEBS-g-MA were used as compatibilizers (Batches E1.3, E1.6). Besides that, using both PP-g-MA and SEBS-g-MA together in the same formulation was another trial (Batch E1.7). In this way, not only the individual effects but also the possible synergistic effects of these materials were examined. The clay content was fixed at 7wt% while using various compatibilizer compositions.

The test results were shown in Table 3.3. The formulation with only PP-g-MA as the compatibilizer yielded slightly higher tensile strength values as compared to neat PP. However the SEBS-g-MA containing formulation had a lower maximum stress value, as seen in Figure 3.3 a and e. Composition with both PP-g-MA and SEBS-g-MA gave a value in between those two, as expected. This order is also valid for Elastic Modulus values (see Figure 3.3c). Stress at yield point values (Figure 3.3e) were increasing when PP-g-MA was used as compatibilizer, however strain at yield values and impact values (Figure 3.3f) were increasing when the coupling agent was SEBS-g-MA. As shown in Figure 3.3b, e and f, nanocomposites with SEBS-g-MA had better strain at maximum force and impact properties compared to other specimens. Work up to maximum force values (see Figure

3.3d) were also related to ductility behavior of the material hence it gave similar results as strain results.

Weld-line tensile specimens, naturally, gave lower values but they have almost the same trends with tensile test results.

Table 3.3. Nanocomposite mechanical test results with respect to compatibilizer type (The standard deviations are given in parenthesis).

	PP	**E1.3**	**E1.6**	**E1.7**
Max Stress [MPa]	33.25 (1.02)	34.10 (0.27)	23.19 (0.09)	29.46 (0.26)
Max Stress [MPa] (Weld-line tensile test)	31.71 (0.35)	18.22 (0.46)	16.93 (0.17)	20.32 (0.78)
Strain at F_{max} [%]	9.05 (0.14)	6.92 (0.17)	11.46 (0.30)	9.27 (0.11)
Strain at F_{max} [%] (Weld-line tensile test)	8.96 (0.19)	1.24 (0.03)	3.91 (0.38)	2.60 (0.21)
E Modulus [MPa]	1429.07 (125.98)	2021.10 (41.24)	1000.23 (70.96)	1424.49 (34.61)
E Modulus [MPa] (Weld-line tensile test)	1454.75 (78.72)	1877.13 (57.65)	906.32 (60.73)	1330.52 (52.25)
E Modulus [MPa] (Flexural test)	1298.75 (54.30)	1655.79 (17.93)	918.17 (34.11)	1138.67 (17.31)
Work up to F_{max} [Nmm]	5052.76 (145.93)	3982.55 (109.24)	4659.42 (114.15)	4717.08 (40.79)
Work up to F_{max} [Nmm] (Weld-line tensile test)	4860.15 (170.35)	272.82 (10.58)	912.06 (82.45)	712.63 (98.58)
Stress at Yield [MPa] (Flexural test)	38.84 (0.56)	42.53 (0.20)	29.81 (0.35)	35.22 (0.14)
Strain at Yield [%] (Flexural test)	7.29 (0.15)	7.06 (0.17)	7.55 (0.11)	7.70 (0.07)
Impact Strength [kJ/m^2]	2.89 (0.16)	3.46 (0.24)	7.10 (0.59)	3.38 (0.26)

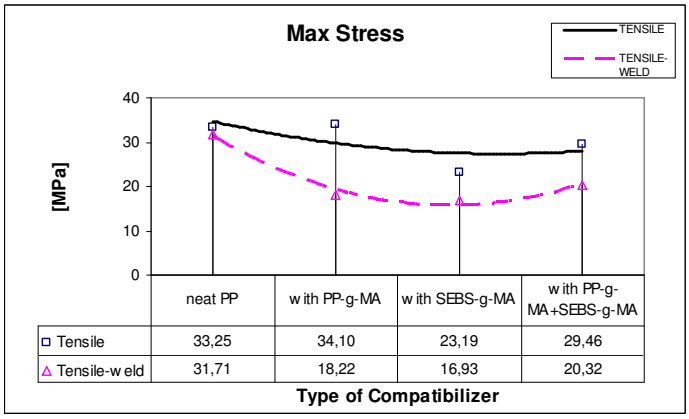

(a) Maximum stress values

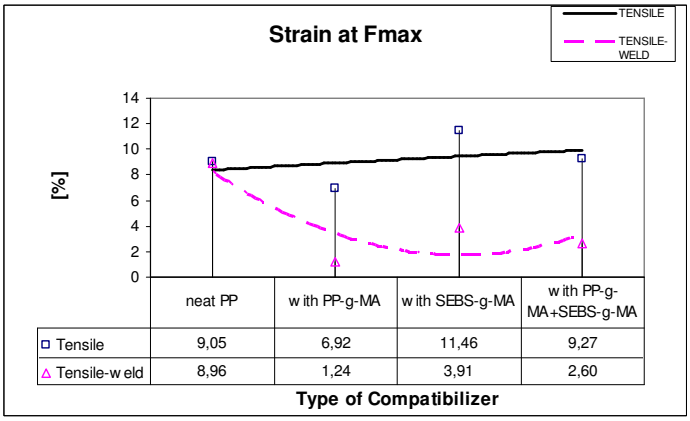

(b) Strain at maximum force values

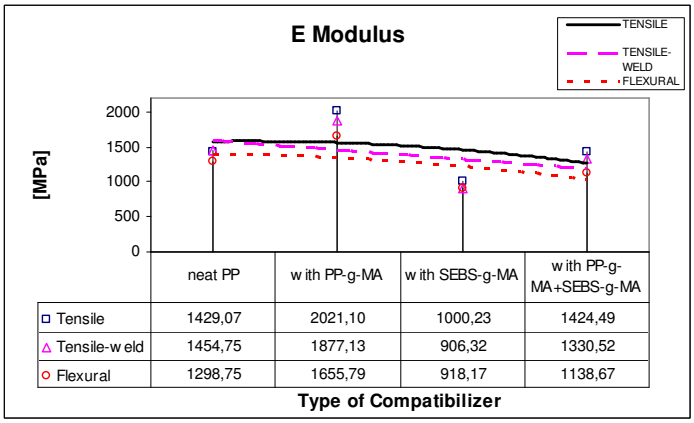

(c) Elastic modulus values

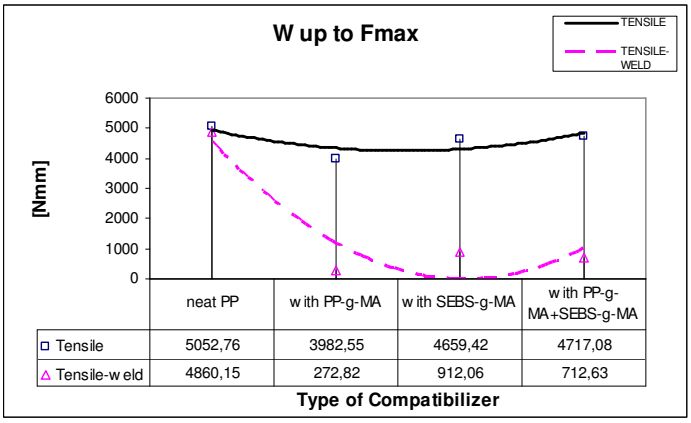

(d) Work up to maximum force values

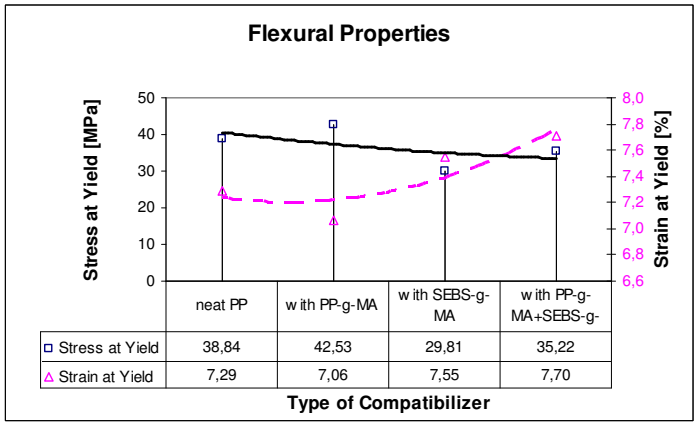

(e) Flexural test values

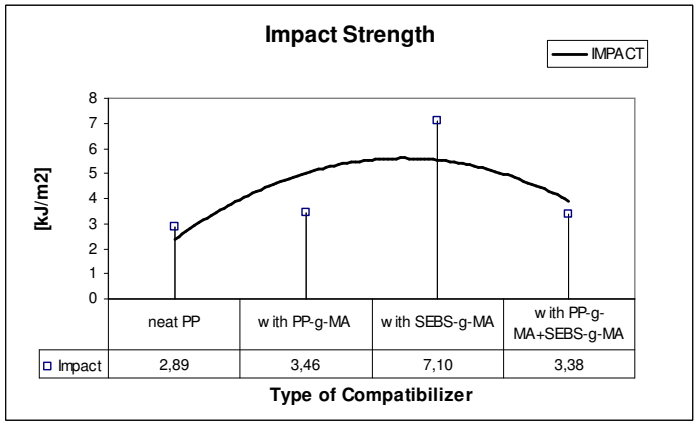

(f) Izod-impact test values

Figure 3.3. Nanocomposite mechanical test results with respect to compatibilizer type, (a) Maximum stress values, (b) Strain at maximum force values, (c) Elastic modulus values, (d) Work up to maximum force values, (e) Flexural test values, (f) Izod-impact test values

These test results proved that nanocomposites containing PP-g-MA had slightly higher strength properties, while nanocomposites with SEBS-g-MA were more ductile. This was expected since styrene-ethylene-butylene-styrene (SEBS) had a rubber characteristic and that increased the elasticity of the compound. Considering those test results, a recipe by using both compatibilizers was prepared. Improving the tensile strength was the most important criteria in this study so the PP-g-MA content should be higher than SEBS-g-MA. However, SEBS-g-MA was needed to increase the ductility and strain at maximum force properties. An optimum ratio (15wt% PP-g-MA and 6wt% SEBS-g-MA) was decided to obtain an optimum reinforcement in the nanocomposite. Here, total ratio of the compatibilizers was fixed at 21wt%. This composition including the two coupling agents was used in further experiments related to process conditions.

3.2.3. Nanocomposite Properties with respect to Screw Speed

Dispersion of nanoclay layers in the polymer can be obtained by both chemical and mechanical processes. Determining the nanocomposite formulation by varying the clay content and compatibilizer type affects the chemical processes and the conditions during manufacturing process affects mechanical processes. Shear rate and residence time are the main process parameters that affect on the dispersion of the clay and they can be controlled by changing the screw parameters of the extruder.

In this work, three different screw speed values were used and compared to each other to determine the effects of extrusion parameters on the dispersion of clay into the polymer (see Table 3.4 and Figure 3.4).

The experiments made so far were all had a screw speed value of 500 rpm. In this set of experiments (E2.1, E2.2, and E2.3), 300 rpm and 100 rpm values were tried in addition to 500 rpm. The specimen prepared at 500 rpm with no filler (E1.8) was also included to the comparison. As shown in Figure 3.4a, c, e and f, maximum stress values and elastic modulus of the nanocomposite were increasing slightly but the impact strength remained almost the same. Strain properties and work up to maximum force values showed little decrease (see Figure 3.4b and d). The blank nanocomposite (with no filler) showed almost the same mechanical properties with the one with filler at 500 rpm. Weld-line tensile test

results had again lower values but similar trends except maximum stress and strain values and toughness curves. Ductility properties of the weld-line specimens dramatically decreased compared to neat PP and blank batch (E1.8) due to the weld line effect which causes a quick rupture of the sample. The formulation was constant at each trial (72wt% PP + 15wt% PP-g-MA + 6wt% SEBS-g-MA + 7wt% Nanofiller) except batch E1.8.

Table 3.4. Nanocomposite mechanical test results with respect to screw speed (The standard deviations are given in parenthesis).

	PP	**E1.8**	**E2.1**	**E2.2**	**E2.3**
Max Stress [MPa]	33.25 (1.02)	29.78 (0.41)	28.36 (0.47)	29.02 (0.31)	29.40 (0.27)
Max Stress [MPa] (Weld-line tensile test)	31.71 (0.35)	26.42 (0.20)	20.80 (0.14)	20.24 (0.21)	18.59 (0.54)
Strain at F_{max} [%]	9.05 (0.14)	9.46 (0.07)	9.51 (0.19)	9.24 (0.14)	9.15 (0.06)
Strain at F_{max} [%] (Weld-line tensile test)	8.96 (0.19)	5.81 (0.13)	2.71 (0.03)	2.42 (0.06)	2.04 (0.14)
E Modulus [MPa]	1429.07 (125.98)	1372.04 (46.58)	1395.41 (22.19)	1477.99 (39.87)	1480.45 (50.57)
E Modulus [MPa] (Weld-line tensile test)	1454.75 (78.72)	1219.99 (66.42)	1390.03 (24.72)	1395.63 (58.67)	1396.88 (67.86)
E Modulus [MPa] (Flexural test)	1298.75 (54.30)	1129.12 (43.50)	1204.45 (40.94)	1214.64 (11.61)	1198.92 (36.05)
Work up to F_{max} [Nmm]	5052.76 (145.93)	4801.82 (75.41)	4673.23 (84.34)	4640.31 (57.70)	4652.44 (44.41)
Work up to F_{max} [Nmm] (Weld-line tensile test)	4860.15 (170.35)	2410.90 (72.56)	761.14 (18.34)	642.73 (20.49)	483.56 (53.21)
Stress at Yield [MPa] (Flexural test)	38.84 (0.56)	34.41 (0.38)	36.25 (0.58)	37.71 (0.10)	37.29 (0.46)
Strain at Yield [%] (Flexural test)	7.29 (0.15)	7.45 (0.17)	7.78 (0.23)	7.97 (0.54)	7.88 (0.22)
Impact Strength [kJ/m^2]	2.89 (0.16)	3.75 (0.05)	3.62 (0.16)	3.43 (0.22)	3.40 (0.22)

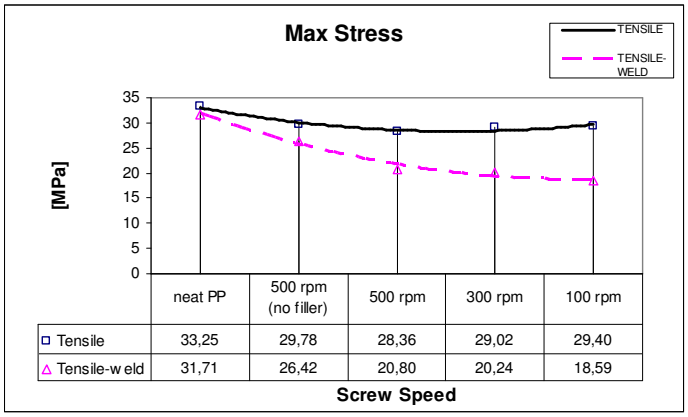

	neat PP	500 rpm (no filler)	500 rpm	300 rpm	100 rpm
Tensile	33,25	29,78	28,36	29,02	29,40
Tensile-weld	31,71	26,42	20,80	20,24	18,59

(a) Maximum stress values

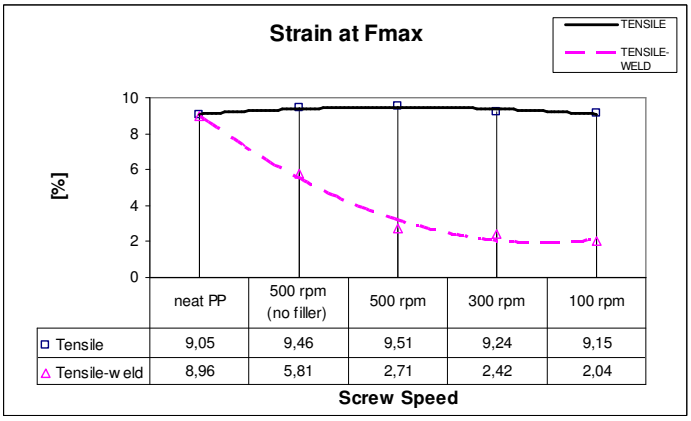

	neat PP	500 rpm (no filler)	500 rpm	300 rpm	100 rpm
Tensile	9,05	9,46	9,51	9,24	9,15
Tensile-weld	8,96	5,81	2,71	2,42	2,04

(b) Strain at maximum force values

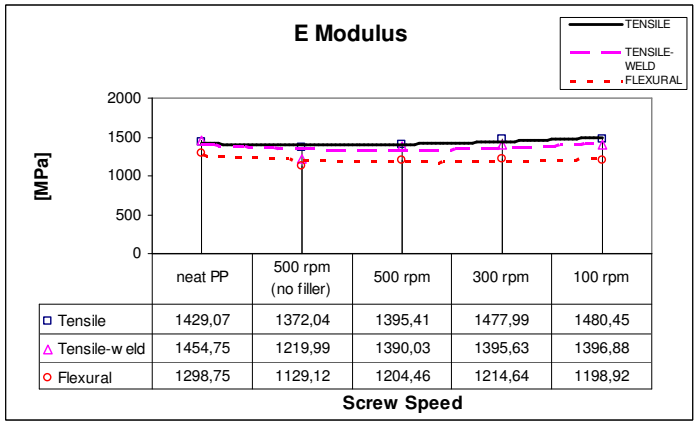

	neat PP	500 rpm (no filler)	500 rpm	300 rpm	100 rpm
Tensile	1429,07	1372,04	1395,41	1477,99	1480,45
Tensile-weld	1454,75	1219,99	1390,03	1395,63	1396,88
Flexural	1298,75	1129,12	1204,46	1214,64	1198,92

(c) Elastic modulus values

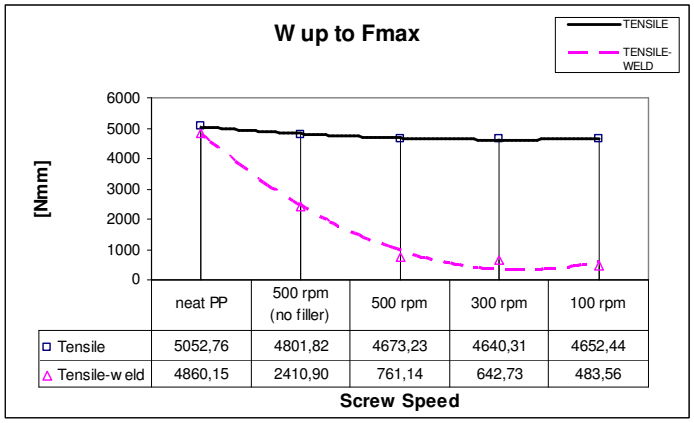

(d) Work up to maximum force values

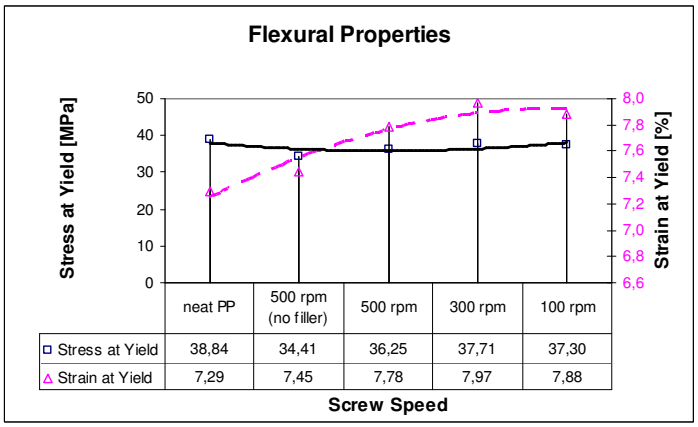

(e) Flexural test values

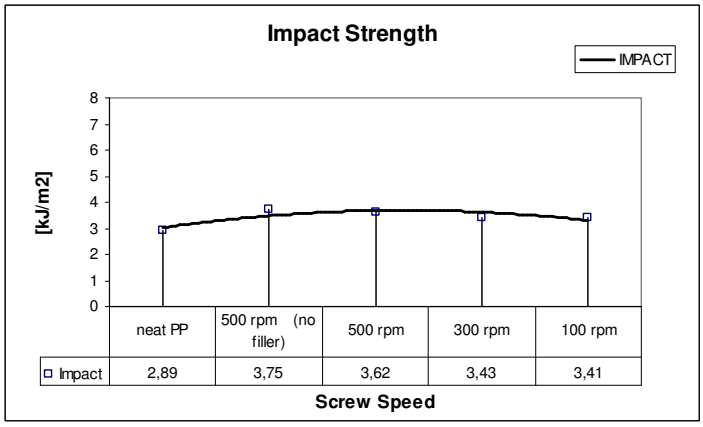

(f) Izod-impact test values

Figure 3.4. Nanocomposite mechanical test results with respect to screw speed, (a) Maximum stress values, (b) Strain at maximum force values, (c) Elastic modulus values, (d) Work up to maximum force values, (e) Flexural test values, (f) Izod-impact test values

High shear rates provide better clay dispersion but also may reduce the strength of the nanocomposite by lowering the aspect ratio of the clay layers by breakage. However with insufficient shear rates, it may not be possible to obtain a well dispersion. Here, lowering the screw speed from 500 rpm to 100 rpm increased the residence time and decreased the shear force. According to the test results, nanocomposites prepared at 100 rpm gave slightly better results compared to the other samples according to tensile test results, thus 100 rpm can be considered as the optimum screw speed value.

Specific Mechanical Energy (SME) is a value that gives the energy consumption per kilogram. Using the formulation below, SME values for experiments with different screw speeds were calculated approximately.

$$SME = \frac{\frac{ScrewSpeed}{MaxSpeed} \times \frac{\%Torque}{100\%} \times MotorPower}{LineOutput}$$

SME value was 0.24 [kWh/kg] for the experiment with 500 rpm (E2.1), 0.25 [kWh/kg] for 300 rpm (E2.2) and 0.14 [kWh/kg] for 100 rpm (E2.3). Manufacturing at 100 rpm seems the most economical choice.

3.2.4. Nanocomposite Properties with respect to Screw Design

Shear rate and residence time parameters of the process can also be adjusted by the screw design. The screws of the extruder used were modular and two different screw configurations were tried. One of them was the screw used so far which had a high shear rate (Batch E2.1). The other configuration was designed to lower the shear rate (Batch E2.4). The formulation of the nanocomposite was kept constant, as the same as the previous trial and the screw speed was fixed at 100 rpm. Batch E1.8 which was compounded at 500 rpm and by high shear screw without filler was also compared with those specimens.

The effects of screw design on the mechanical properties of the nanocomposite were shown in Table 3.5 and Figure 3.5. When medium shear (MS) screw is used instead of high shear (HS) screw, a slight increase in maximum stress, elastic modulus and impact values and a decrease in strain values were obtained according to tensile test results (see

Figure 3.5a, b, c, d, e and f). The batch without filler showed slightly higher ductility properties than those with filler, as expected.

Table 3.5. Nanocomposite mechanical test results with respect to screw design (The standard deviations are given in parenthesis).

	PP	**E1.8**	**E2.3**	**E2.4**
Max Stress [MPa]	33.25 (1.02)	29.78 (0.41)	29.40 (0.27)	30.06 (0.23)
Max Stress [MPa] (Weld-line tensile test)	31.71 (0.35)	26.42 (0.20)	18.59 (0.54)	18.43 (0.25)
Strain at F_{max} [%]	9.05 (0.14)	9.46 (0.07)	9.15 (0.06)	8.42 (0.14)
Strain at F_{max} [%] (Weld-line tensile test)	8.96 (0.19)	5.81 (0.13)	2.04 (0.14)	1.62 (0.03)
E Modulus [MPa]	1429.07 (125.98)	1372.04 (46.58)	1480.45 (50.57)	1644.79 (52.26)
E Modulus [MPa] (Weld-line tensile test)	1454.75 (78.72)	1219.99 (66.42)	1396.88 (67.86)	1586.50 (86.45)
E Modulus [MPa] (Flexural test)	1298.75 (54.30)	1129.12 (43.50)	1198.92 (36.05)	1212.60 (32.44)
Work up to F_{max} [Nmm]	5052.76 (145.93)	4801.82 (75.41)	4652.44 (44.41)	4363.06 (91.39)
Work up to F_{max} [Nmm] (Weld-line tensile test)	4860.15 (170.35)	2410.90 (72.56)	483.56 (53.21)	364.09 (13.79)
Stress at Yield [MPa] (Flexural test)	38.84 (0.56)	34.41 (0.38)	37.29 (0.46)	38.08 (0.78)
Strain at Yield [%] (Flexural test)	7.29 (0.15)	7.45 (0.17)	7.88 (0.22)	7.56 (0.09)
Impact Strength [kJ/m^2]	2.89 (0.16)	3.75 (0.05)	3.40 (0.22)	3.69 (0.28)

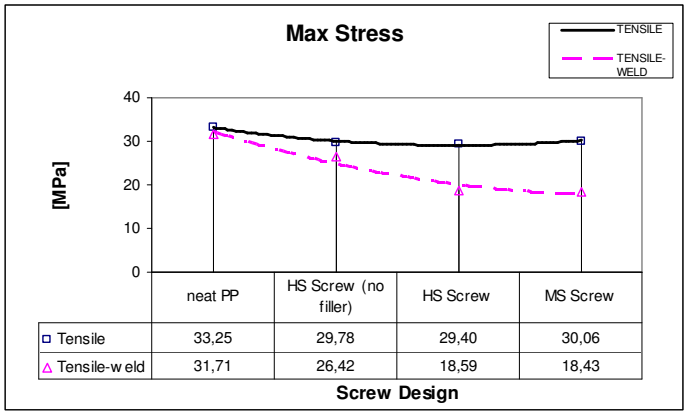

(a) Maximum stress values

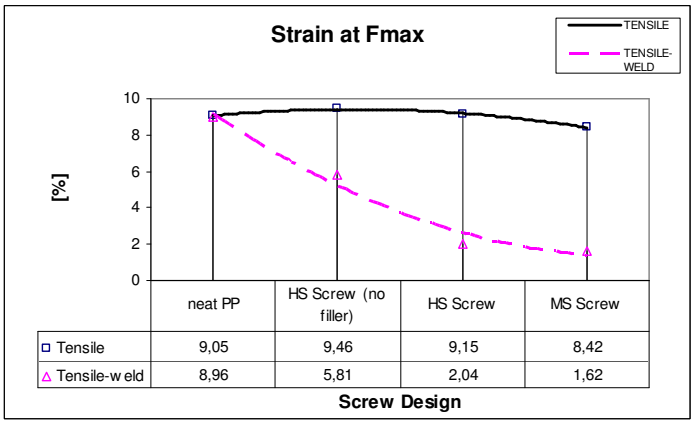

(b) Strain at maximum force values

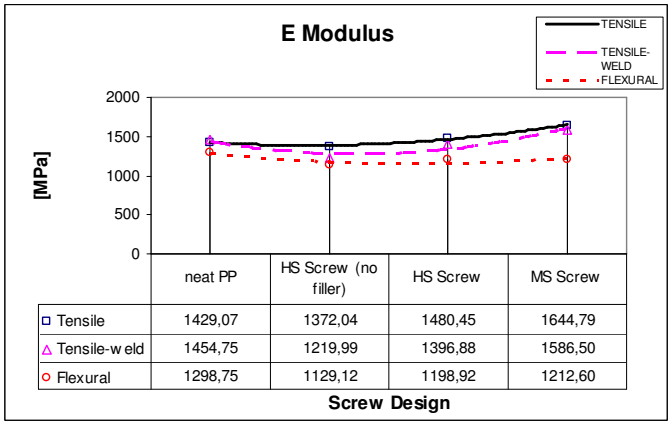

(c) Elastic modulus values

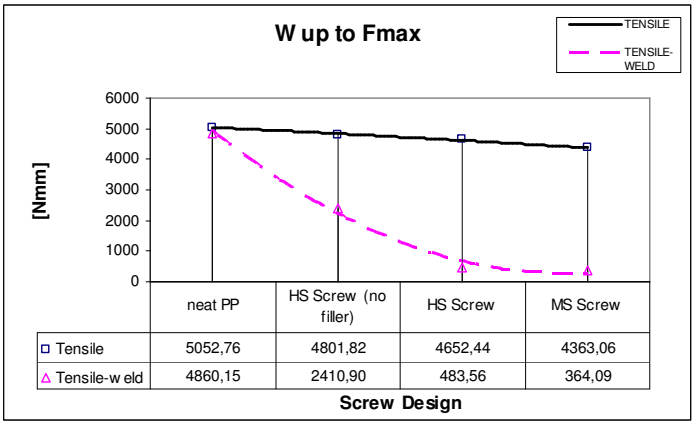

(d) Work up to maximum force values

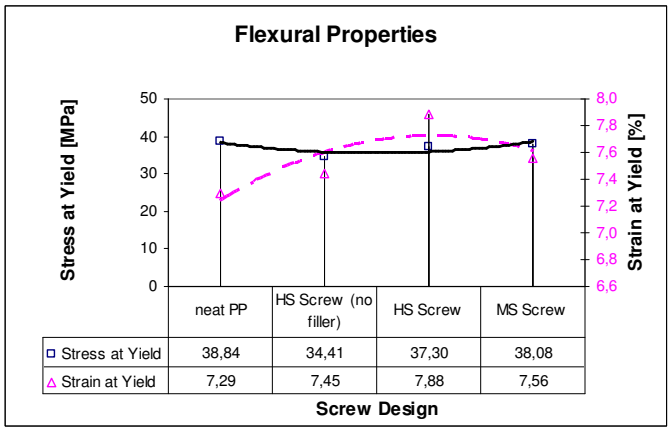

(e) Flexural test values

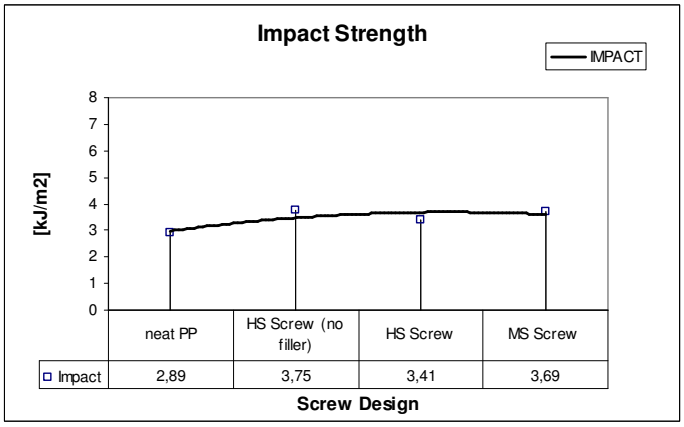

(f) Izod-impact test values

Figure 3.5. Nanocomposite mechanical test results with respect to screw design, (a) Maximum stress values, (b) Strain at maximum force values, (c) Elastic modulus values, (d) Work up to maximum force values, (e) Flexural test values, (f) Izod-impact test values

Mechanical properties were improved with lowering the shear rate. This could be explained by the clay aspect ratio assumption mentioned before. A medium shear screw produced adequate shear rate to disperse the clay well.

3.2.5. Nanocomposite Properties with respect to Loading Order

The main problem in preparing nanocomposites was obtaining well dispersion of clay in the polymer matrix. Several trials by varying the formulation and shear rate were made to enhance the interaction between the nanofiller and the polymer matrix. The method used so far was using the two compatibilizers together in the recipe (15wt% PP-g-MA and 6wt% SEBS-g-MA) and dry blending these two components with PP before loading into the extruder feeder. By this way, the polymer and the compatibilizer granules were blended manually before fed into the extruder but it was hard to distinguish the individual effects of these coupling agents in the compound. It was not clear that in which phase the nanoclay resides. Hence, in this set of trials, the purpose was to distinguish the phase which hydrophilic nanoclay prefers. For this purpose the compatibilizers were blended sequentially and in differing orders. Preparation of these batches was explained in detail in the Experimental Procedure section. The mechanical test results of the PP-g-MA-first blended compound (E 2.5), the SESB-g-MA-first blended compound (E 2.7) and the final forms of those compounds (E 2.6 and E 2.8) were shown in Table 3.6 and Figure 3.6. The batch in which the two compatibilizers were pre-blended before loading (E2.3) and the batch prepared with the same method but without filler (E1.8) were also included to comparison. The screw speed was fixed at 100 rpm except the batch E1.8 which was compounded at 500 rpm.

Table 3.6. Nanocomposite mechanical test results with respect to loading order (The standard deviations are given in parenthesis).

	PP	**E1.8**	**E2.3**	**E2.5**	**E2.6**	**E2.7**	**E2.8**
Max Stress [MPa]	33.25 (1.02)	29.78 (0.41)	29.40 (0.27)	33.04 (0.16)	30.15 (0.11)	29.29 (0.19)	30.41 (0.22)
Max Stress [MPa] (Weld-line tensile)	31.71 (0.35)	26.42 (0.20)	18.59 (0.54)	17.94 (0.36)	19.42 (0.63)	18.39 (0.29)	19.97 (0.40)
Strain at F_{max} [%]	9.05 (0.14)	9.46 (0.07)	9.15 (0.06)	7.00 (0.03)	8.96 (0.07)	8.65 (0.06)	8.76 (0.14)
Strain at F_{max} [%] (Weld-line tensile)	8.96 (0.19)	5.81 (0.13)	2.04 (0.14)	1.28 (0.04)	1.94 (0.13)	1.88 (0.07)	2.09 (0.09)
E Modulus [MPa]	1429.07 (125.98)	1372.04 (46.58)	1480.45 (50.57)	1904.95 (31.69)	1513.56 (28.91)	1568.65 (74.36)	1540.74 (30.00)
E Modulus [MPa] (Weld-line tensile)	1454.75 (78.72)	1219.99 (66.42)	1396.88 (67.86)	1855.73 (48.15)	1493.73 (72.48)	1447.59 (41.94)	1460.27 (48.93)
E Modulus [MPa] (Flexural test)	1298.75 (54.30)	1129.12 (43.50)	1198.92 (36.05)	1397.79 (45.60)	1114.40 (23.62)	1041.23 (33.99)	1149.65 (53.28)
Work up to F_{max} [Nmm]	5052.76 (145.93)	4801.82 (75.41)	4652.44 (44.41)	3882.69 (15.41)	4651.63 (54.03)	4393.62 (29.88)	4556.41 (50.40)
Work up to F_{max} [Nmm] (Weld-line tensile)	4860.15 (170.35)	2410.90 (72.56)	483.56 (53.21)	279.43 (16.19)	472.00 (49.07)	435.79 (23.71)	536.63 (39.43)
Stress at Yield [MPa] (Flexural test)	38.84 (0.56)	34.41 (0.38)	37.29 (0.46)	44.10 (0.40)	37.31 (0.43)	34.70 (0.92)	35.47 (0.17)
Strain at Yield [%] (Flexural test)	7.29 (0.15)	7.45 (0.17)	7.88 (0.22)	7.82 (0.45)	7.81 (0.30)	7.44 (0.21)	7.50 (0.22)
Impact Strength [kJ/m^2]	2.89 (0.16)	3.75 (0.05)	3.40 (0.22)	3.32 (0.21)	3.99 (0.18)	3.19 (0.14)	3.62 (0.23)

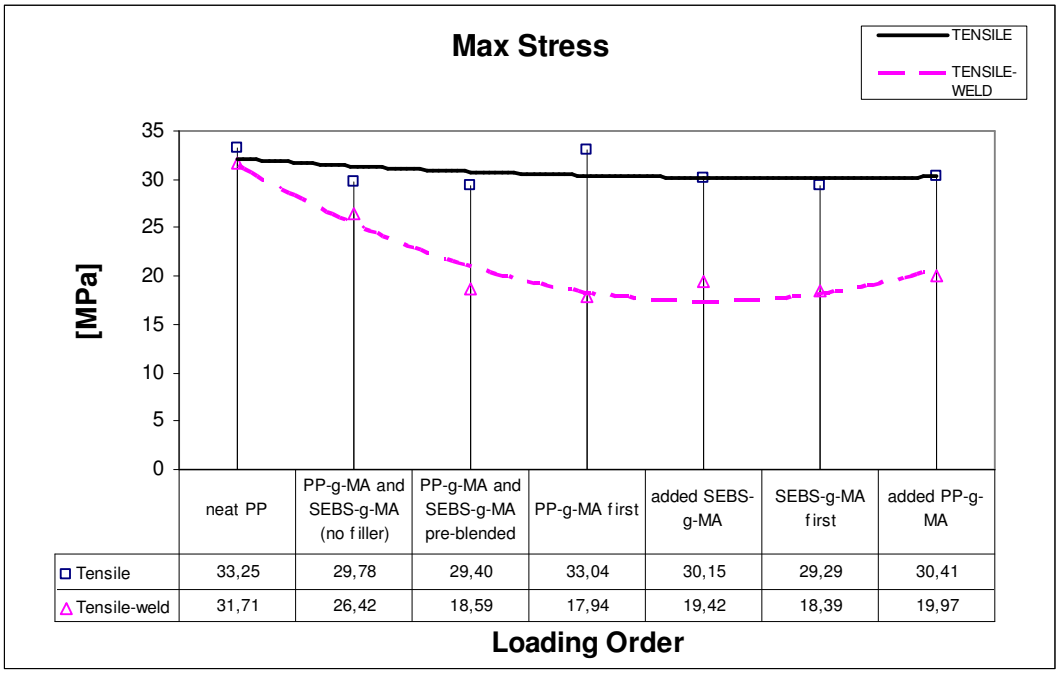

	neat PP	PP-g-MA and SEBS-g-MA (no filler)	PP-g-MA and SEBS-g-MA pre-blended	PP-g-MA first	added SEBS-g-MA	SEBS-g-MA first	added PP-g-MA
Tensile	33,25	29,78	29,40	33,04	30,15	29,29	30,41
Tensile-weld	31,71	26,42	18,59	17,94	19,42	18,39	19,97

(a) Maximum stress values

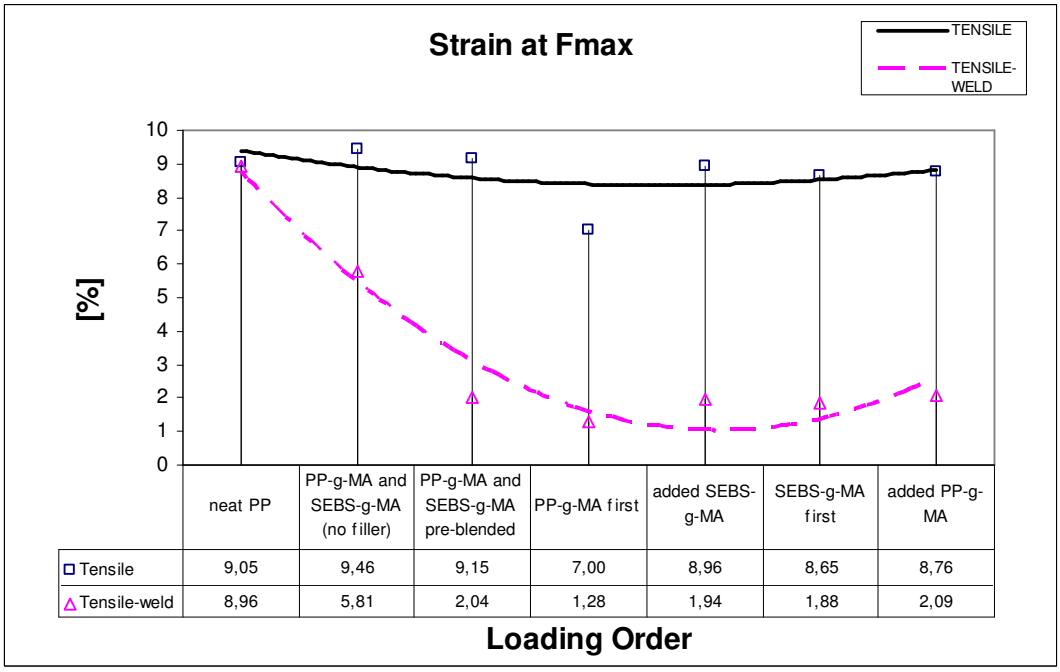

	neat PP	PP-g-MA and SEBS-g-MA (no filler)	PP-g-MA and SEBS-g-MA pre-blended	PP-g-MA first	added SEBS-g-MA	SEBS-g-MA first	added PP-g-MA
Tensile	9,05	9,46	9,15	7,00	8,96	8,65	8,76
Tensile-weld	8,96	5,81	2,04	1,28	1,94	1,88	2,09

(b) Strain at maximum force values

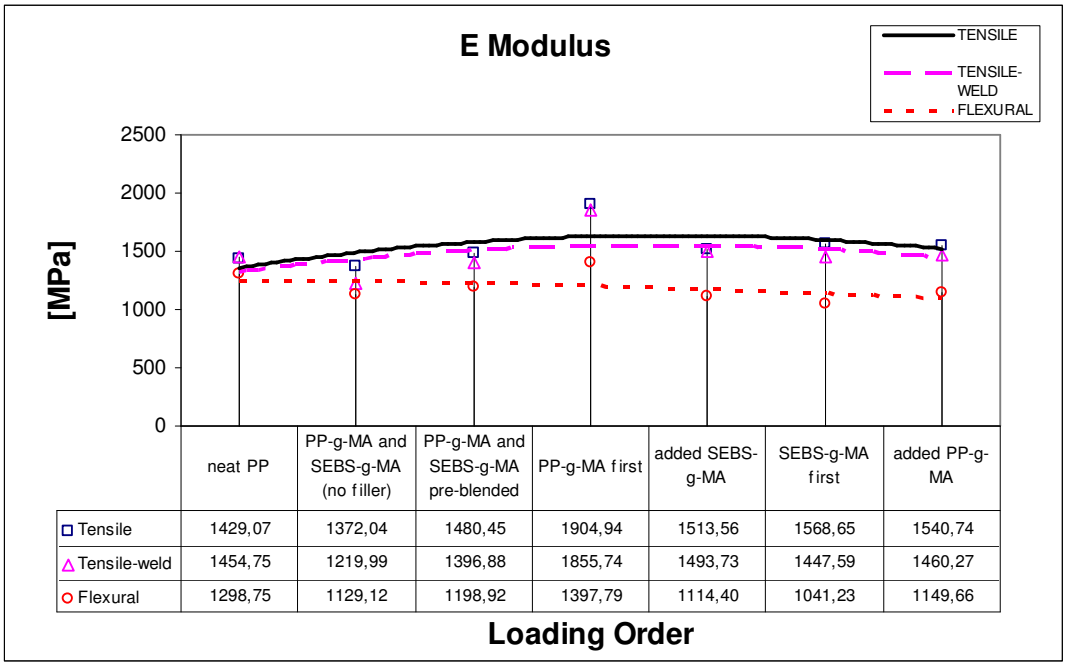

	neat PP	PP-g-MA and SEBS-g-MA (no filler)	PP-g-MA and SEBS-g-MA pre-blended	PP-g-MA first	added SEBS-g-MA	SEBS-g-MA first	added PP-g-MA
Tensile	1429,07	1372,04	1480,45	1904,94	1513,56	1568,65	1540,74
Tensile-weld	1454,75	1219,99	1396,88	1855,74	1493,73	1447,59	1460,27
Flexural	1298,75	1129,12	1198,92	1397,79	1114,40	1041,23	1149,66

(c) Elastic modulus values

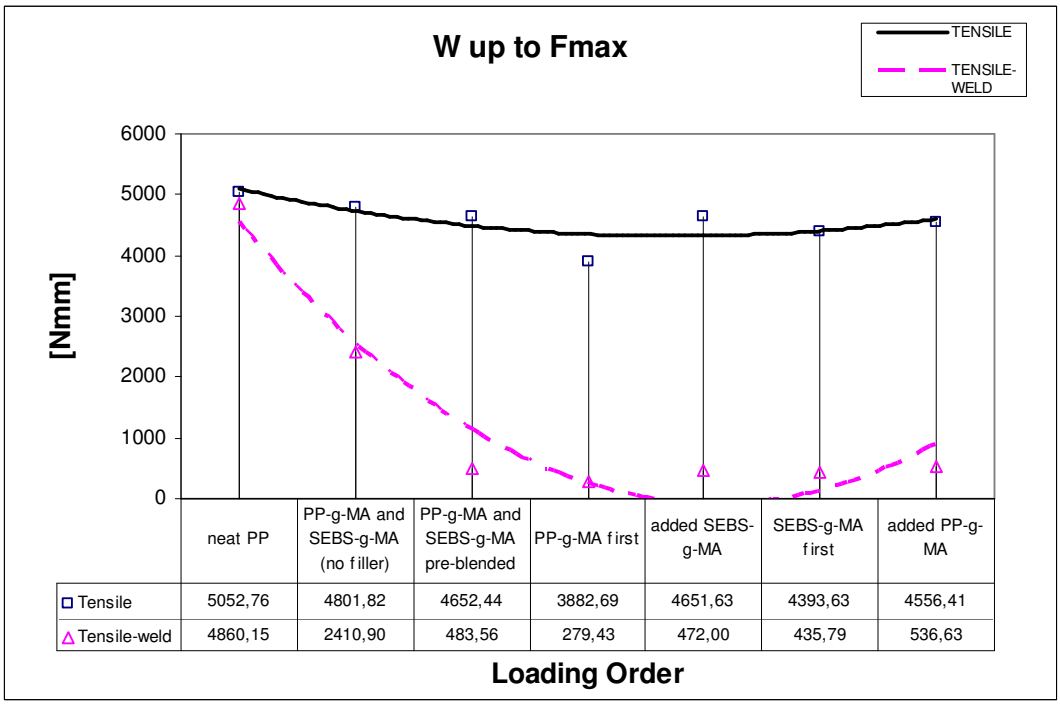

	neat PP	PP-g-MA and SEBS-g-MA (no filler)	PP-g-MA and SEBS-g-MA pre-blended	PP-g-MA first	added SEBS-g-MA	SEBS-g-MA first	added PP-g-MA
Tensile	5052,76	4801,82	4652,44	3882,69	4651,63	4393,63	4556,41
Tensile-weld	4860,15	2410,90	483,56	279,43	472,00	435,79	536,63

(d) Work up to maximum force values

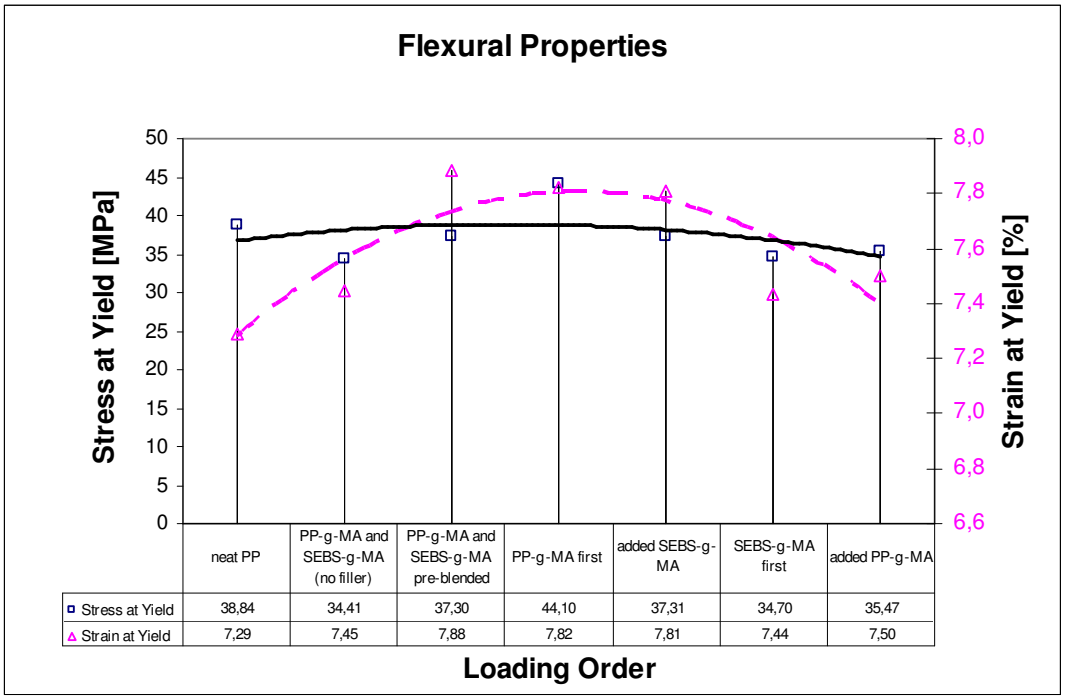

(e) Flexural test values

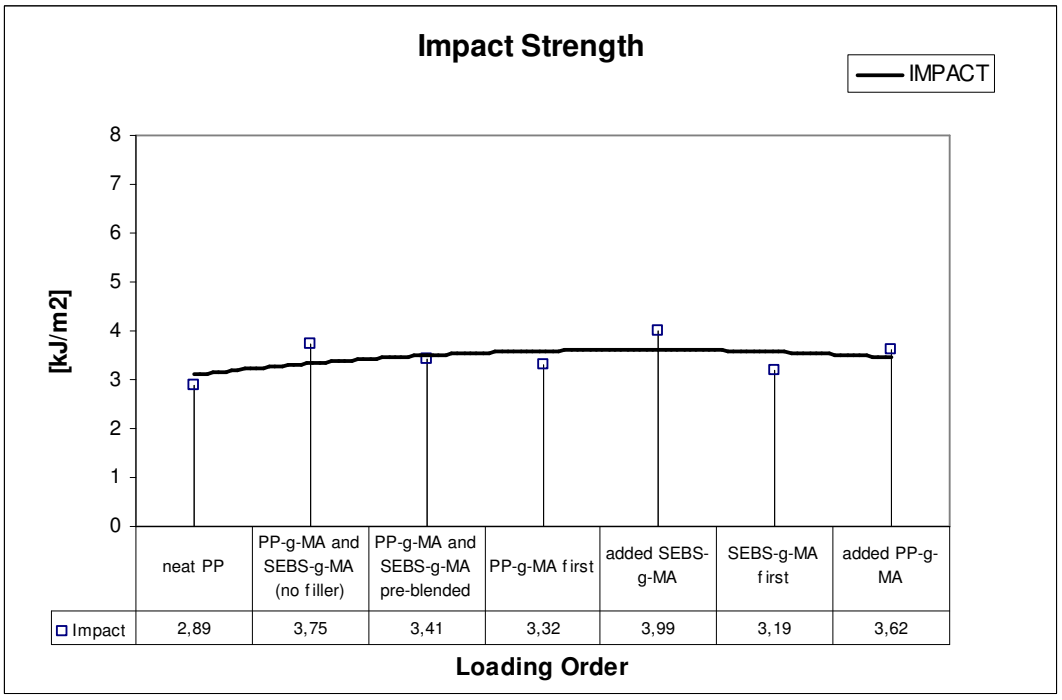

(f) Izod-impact test values

Figure 3.6. Nanocomposite mechanical test results with respect to loading order, (a) Maximum stress values, (b) Strain at maximum force values, (c) Elastic modulus values, (d) Work up to maximum force values, (e) Flexural test values, (f) Izod-impact test values

Maximum stress value and the elastic modulus were reduced by SEBS-g-MA addition (see Figure 3.6a, c and e) but in contrast; maximum strain and work up to maximum force values showed an increase (see Figure 3.6b and d). This was due to the rubber characteristic of SEBS. On the other hand, PP-g-MA had an effect on improving the tensile strength and also the strain properties of the nanocomposite. Impact strength of the material was improved by either PP-g-MA or SEBS-g-MA addition as shown in Figure 3.6f. The blank batch (without filler) showed slightly higher strain properties but lower strength properties than the batches with nanofiller due to the rubber characteristic of the compatibilizer. Another possible explanation is the inefficiency of the filler a reinforcement due to low exfoliation. A remarkable point that should be reported was that, by changing the loading order of the compatibilizers, stress, elastic modulus and impact strength values showed little increase while strain values slightly reduced.

Loading order did not have significant effects on the mechanical properties of the nanocomposites. Compounding PP-g-MA at first increased the strength but reduced the ductility. SEBS-g-MA addition to this mixture; this time, increased the ductility but decreased the strength properties. The final batches prepared with different loading order had almost the same mechanical properties with the batch prepared by pre-blending of the compatibilizers. According to these results no significant effect on mechanical properties was observed due to nanoclay dispersion in the discrete rubber and polypropylene phases.

3.3. Summary of the Results Obtained

- The clay/compatibilizer ratio was fixed, hence when the clay content was increased, the compatibilizer content was also increased. Due to this raise, nanocomposites with PP-g-MA became more brittle but not tough enough. In contrast, ductility of nanocomposites with SEBS-g-MA were increased which was attributable to the increase in rubber content. It is also remarkable that according to XRD analysis nanocomposites including PP-g-MA showed signs of exfoliation where the nanocomposites compatibilized by SEBS-g-MA were well exfoliated.

- Using PP-g-MA as the compatibilizer increased the strength properties of the nanocomposite. On the other hand, nanocomposites with SEBS-g-MA were more

ductile and impact resistant due to the rubber content. The main criterion of this study was improving tensile strength without loss of ductility. To obtain an optimum mechanical property, these two compatibilizers were used in the same formulation with an optimum content. This new recipe also increased the gallery spacing significantly.

- Rotational speed of the extruder screws has a significant effect on the shear rate which is related to the dispersion of clay layers. High shear rates provide better clay dispersion but also may reduce the strength of the nanocomposite by lowering the aspect ratio of the clay layers by breakage of individual flakes. Here, lower screw speed slightly increased the strength properties. All the nanocomposites with different screw speed values were well intercalated with increased gallery spacing values.

- Design of the modular screws was another significant property that affects the shear rate. In this study two screw configurations were tried to examine the shear effect. Strength properties of the nanocomposites slightly increased when shear rate is reduced. This is probably due to the aspect ratio assumption. A medium shear screw produced adequate shear rate to disperse clay well.

- Compatibilizers were dry blended before loading into extruder feeder. By this way it was hard to distinguish the individual effects of the compatibilizers and the phase in which nanoclay resides. In this trial, compatibilizers were blended one by one and in differing orders. PP-g-MA addition increased the strength properties while ductility was increased by the addition of SEBS-g-MA. According to the global results, differing the loading order of the compatibilizers slightly increased the strength properties but did not affect mechanical properties significantly.

- Weld-line tensile test results showed more or less similar trends with tensile test results for elastic modulus values. However, maximum stress values were decreasing slightly and the strain and toughness properties were decreasing dramatically compared to neat PP and the blank batch. The weld line in the midpoint of the tensile specimen reduces the durability of the nanocomposite and those specimens rupture without any significant elongation.

4. CONCLUSION AND FUTURE WORK

Polymeric nanocomposite technology is a new era with a huge area of research. Especially in our country there has been not much research and publications on nanocomposites yet. This study was an experimental approach to polymeric nanocomposite world. The question was with which content and at which conditions the nanocomposites provide enhanced physical and mechanical properties.

Polypropylene (PP) as the base polymer and organo-modified montmorillonite (OMMT) as the nanofiller was the components used with two types of compatibilizers. Melt intercalation method was applied by an intermeshing co-rotating twin screw extruder. First trials were to obtain a recipe providing enhanced properties and then by using that formulation at various conditions, mechanical reinforcement of the nanocomposites were aimed.

Compatibilizer type and content affected most on the nanocomposite structure and strength. PP-g-MA had an effect to increase strength and SEBS-g-MA was better at improving ductility. Using them both in the compound with an optimum content optimized the mechanical improvement due to their synergistic effects.

Dispersing clay in the PP matrix was the main point to obtain both physical and mechanical improvement. Process parameters were keys for better dispersion of clay layers. By varying screw speed and screw design in the extruder, different shear profiles were tried. Higher shear rates provided better dispersion by breaking up the clay agglomerates, however excessive shear rate had negatives effects on strength of the nanocomposite since the clay platelets could have been shattered. Processing with lower screw speed and with a medium shear screw instead of high shear, provided better mechanical results.

The individual effects of the compatibilizers in the formulation and the discrete phases in which nanoclay may reside were not clear, hence loading the compatibilizers

sequentially was tried. As the results of the tests, there was only little enhancement in mechanical properties by varying the loading order of the compatibilizers in the extruder.

As a consequence, according to the results of the experiments carried out, the effects of the raw material properties and the formulation were more significant on reinforcement compared to the effects of processing conditions. The conditions for nanocomposite preparation are effective only when the good interaction between the components of the nanocomposite is achieved. Optimized processing parameters used with effective compounding materials content, the better clay delamination and improved properties would be obtained.

As a future work, loading some of the compounds from downstream, from a different barrel may be a different trial about melting characteristic of the compound. Polymer diffusion into the clay galleries could be enhanced by this way. The most crucial point that has to be carried out is the transmission electron microscopy (TEM) analysis that informs much about nanostructure of the nanocomposite. This kind of analysis will bring out the clay dispersion in discrete phases and may also explain the reduction in strength due to reduction of aspect ratio by breakage of individual layers in batches prepared with high shear. TEM will be a complementary study to XRD analysis since it is not clear whether the clay layers are dispersed individually or they are shattered in the polymer matrix by only XRD curves. TEM micrographs will probably make these structure visible.

REFERENCES

1. Fukushima, Y., A. Okada, M. Kawasumi, T. Kurauchi, O. Kamigaito, "Swelling Behaviour of Montmorillonite by Poly-6-Amide", *Clay Miner*, Vol. 23, No. 1, pp. 27-34, 1988

2. Usuki, A., Y. Kojima, M. Kawasumi, A. Okada, Y. Fukushima, T. Kurauchi, "Synthesis of Nylon 6-Clay Hybrid", J. *Mater. Res.*, Vol. 8, No. 5, pp. 1179-1184, 1993

3. Schey, J. A., *Introduction to Manufacturing Processes*, McGraw-Hill Book Company, Singapore, 1987.

4. Ray, S. S. and M. Okamoto, "Polymer/Layered Silicate Nanocomposites: A Review From Preparation to Processing", *Prog. Polym. Sci.*, Vol. 28, pp. 1539-1641, 2003.

5. Li, J., C. Zhou, W. Gang, "Study on Nonisothermal Crystallization of Maleic Anhydride Grafted Polypropylene/Montmorillonite Nanocomposite", *Polymer Testing*, Vol. 22, pp. 217-223, 2003.

6. Dennis, H. R., D. L. Hunter, D. Chang, S. Kim, J. L. White, J. W. Cho, D. R. Paul, "Effect of Melt Processing Conditions on the Extent of Exfoliation in Organoclay-based Nanocomposites", *Polymer*, Vol. 42, pp. 9513-9522, 2001.

7. Pinnavaia, T. J. and G. W. Beall, *Polymer-Clay Nanocomposites*, John Wiley & Sons, Chichester, 2000.

8. Oya, A. and Y. Kurokawa, "Factors Controlling Mechanical Properties of Clay Mineral/Polypropylene Nanocomposites", *J. of Mater. Sci.*, Vol. 35, pp. 1045-1050, 2000.

9. Korakianiti, A., V. Papaefthimiou, T. Daflou, S. Kennou, V. G. Gregoriou, "Characterzation of Polypropylene (PP) Nanocomposites for Industrial Applications", *Macromol. Symp.*, Vol. 205, pp. 71-84, 2004.

10. Pal, S. K. and D. D. Kale, "Effect of Processing Conditions and Properties of PP/Nylon 6 Blends", *J. Polym. Res.*, Vol. 7, No. 2, pp. 107-113, 2000.

11. Szazdi, L., B. Jr. Pukanszky, E. Földes, B. Pukanszky, "Possible Mechanism of Interaction Among the Componennts in MAPP Modified Layered Silicate PP Nanocomposites", *Polymer*, Vol. 46, pp. 8001-8010, 2005.

12. Alexandre, M. and P. Dubois, "Polymer-layered Silicate Nanocomposites: Preparation, Properties and Uses of a New Class of Materials", *Mater. Sci. and Eng.*, Vol. 28, pp. 1-63, 2000.

13. Cho, J. W., and D. R. Paul, "Nylon 6 Nanocomposites by Melt Compounding", *Polymer*, Vol. 42, pp. 1083-1094, 2001.

14. Tjong, S. C. and S. P. Bao, "Fracture Toughness of High Density Polyethylene/SEBS-g-MA/Montmorillonite Nanocomposites", *Composites Science and Technology*, Vol. 67, pp. 314-323, 2007.

15. Lei, S. G., S. V. Hoa, M.-T. Ton-That, "Effect of Clay Types on the Processing and Properties of Polypropylene Nanocomposites", *Composites Science and Technology*, Vol. 66, pp. 1274-1279, 2006.

16. Zhu, L., and M. Xanthos, "Effects of Process Conditions and Mixing Protocols on Structure of Extruded Polypropylene Nanocomposites", *J. Appl. Polym. Sci.*, Vol. 93, pp. 1891-1899, 2004.

17. Kornmann, X., "Synthesis and Caracterisation of Thermoset-Clay Nanocomposites", Division of Polymer Engineering, Lulea University of Technology, Sweeden

18. Benetti, E. M., V. Causin, C. Marega, A. Marigo, G. Ferrrara, A. Ferraro, M. Consalvi, F. Fantinel, "Morphological and Structural Characterization of Polypropylene Based Nanocomposites", *Polymer*, Vol. 46, pp. 8275-8285, 2005.

19. Garcia-Lopez, D., O. Picazo, J. C. Merino, J. M. Pastor, "Polypropylene-Clay Nanocomposites: Effect of Compatibilizing Agents on Clay Dispersion", *European Polymer Journal*; Vol. 39, pp. 945-950, 2003.

20. Usuki, A., M. Kato, A. Okada, T. Kurauchi, "Synthesis of Polypropylene-Clay Hybrid", *J. Appl. Polym. Sci.*, Vol. 63, pp. 137-139, 1997.

21. Kawasumi, M., N. Hasegawa, M. Kato, A. Usuki, A. Okada, "Preparation and Mechanical Properties of Polypropylene-Clay Hybrids", *Macromolecules*, Vol. 30, pp. 6333-6338, 1997.

22. Lertwimolnun, W., and B. Vergnes, "Influence of Compatibilizer and Processing Conditions on the Dispersion of Nanoclay in a Polypropylene Matrix", *Polymer*; Vol. 46, pp. 3462-3471, 2005.

23. Wang, Y., Feng-B. Chen, Kai-C Wu, "Twin-Screw Extrusion Compounding of Polypropylene/Organoclay Nanocomposites Modified by Maleated Polypropylenes", *J. Appl. Polym. Sci.*, Vol. 93, pp. 100-112, 2004.

24. Wang, Y., Feng-B. Chen, Yann-C. Li, Kai-C. Wu, "Melt Processing of Polypropylene/Clay Nanocomposites Modified With Maleated Polypropylene Compatibilizers", *Composites:Part B*, Vol. 35, pp. 111-124, 2004

25. Tjong, S. C., and Y. Z. Meng, "Impact-Modified Polypropylene/Vermiculite Nanocomposites", *J. Polym. Sci.: Part B: Polymer Physics*, Vol. 41, pp. 2332-2341, 2003.

26. Vaia, R. A., H. Ishii, E. P. Giannelis, "Synthesis and Properties of Two-Dimensional Nanostructures by Direct Intercalation of Polymer Melts in Layered Silicates", *Chem. Mater.* Vol. 5, pp. 1694-1696, 1993.

27. Modesti, M., A. Lorenzetti, D. Bon, S. Besco, "Effect of Processing Conditions on Morphology and Mechanical Properties of Compatibilized Polypropylene Nanocomposites", *Polymer*, Vol. 46, pp. 10237-10245, 2005.

28. D. H. Kim, J. U. Park, K. S. Cho, K.H. Ahn, S. J. Lee, "A Novel Fabrication Method for Poly(propylene)/Clay Nanocomposites by Continuous Processing", *Macromol. Mater. Eng.*, Vol. 291, pp. 1127-1135, 2006.

29. Yang, Hong-mei, Yi-hu Song, Bo Xu, Q. Zheng, "Preparation of Exfoliated Low-density Polyethylene/Montmorillonite Nanocomposites Through Melt Extrusion", *Chem. Res. Chinese U.*, Vol. 22(3), pp. 383-387, 2006.

30. Zeus Technical Whitepaper, "Melt Extrusion: The Basic Process", Zeus Industrial Products, Inc., 2006.

31. Rauwendaal, C., *Polymer Extrusion*, Hanser Gardner Publications, Munich, 2001.

32. Raman, V. C., Y. Jaluria, M. V. Karwe, V. Sernas, "Transport in a Twin-Screw Extruder for the Processing of Polymers", *Polym. Eng. Sci.*, Vol. 36, No. 11, pp. 1531-1540, 1996.

33. Prat, L., S. N'Diaye, L. Rigal, C. Gourdon, "Solid-Liquid Transport in a Modified Co-rotating Twin-Screw Extruder_Dynamic Simulator and Experimental Validations", *Chem. Eng. Process.,* Vol. 43, pp. 881-886, 2004.

34. Yoshinaga, M., S. Katsuki, M. Miyazaki, L. Liu, S. I. Kihara, K. Funatsu, "Mixing Mechanism of Three-Tip Kneading Block in Twin Screw Extruders", *Polym. Eng. Sci.*, Vol. 40, No. 1, pp. 168-178, 2000.

35. Tadmor, Z. and S. D. Lipshitz, R. Lavie, “Dynamic Model of a Plasticating Extruder”, *Polym. Eng. Sci.*, Vol. 14, No. 2, pp. 112-119, 1974.

36. Tadmor, Z. and I. Klein, “The Effect of Design and Operationg Conditions on Melting in Plasticating Extruders”, *Polym. Eng. Sci.*, Vol. 9, No. 1, pp. 1-10, 1969.

37. Lertwimolnun, W. and B. Vergnes, “Effect of Processing Conditions on the Formation of Polypropylene/Organoclay Nanocomposites in a Twin Screw Extruder”, *Polym. Eng. Sci.*, Vol. 46, pp. 314-323, 2006.

38. Vainio, T. P., A. Harlin, J. V. Seppala, “Screw Optimization of a Co-Rotating Twin-Screw Extruder for a Binary Immiscible Blend”, *Polym. Eng. Sci.*, Vol. 35, No. 3, pp. 225-232, 1995.

39. Kalyon, D. M. and H. N. Sangani, “An Experimental Study of Distributive Mixing in Fully Intermeshing, Co-Rotating Twin Screw Extruders”, *Polym. Eng. Sci.*, Vol. 29, No. 15, pp. 1018-1026, 1989.

40. Yang, H.-H. and M.-Z. Ica, , “Flow Field Analysis of the Kneading Disc Region in a Co-Rotating Twin Screw Extruder”, *Polym. Eng. Sci.*, Vol. 32, No. 19, pp. 1411-1417, 1992.

41. Shearer, G. and C. Tzoganakis, “The Effect of Kneading Block Design and Operating Conditions on Distributive Mixing in Twin Screw Extruders”, *Polym. Eng. Sci.*, Vol. 40, No. 5, pp. 1095-1106, 2000.

42. Rauwendaal, C., “The Geometry of Self-Cleaning Twin-Screw Extruders”, *Advances in Polymer Technology*, Vol. 15, No. 2, pp. 127-133, 1996

43. Fultz, B. and J. M. Howe, *Transmission Electron Microscopy and Diffractometry of Materials*, Springer, Germany, 2002

44. Treece, M. A., W. Zhang, R. D. Moffitt, J. P. Oberhauser, "Twin-Screw Extrusion of Polypropylene-Clay Nanocomposites: Influence of Masterbatch Processing, Screw Rotation Mode and Sequence", *Polym. Eng. Sci.*, Vol. 47, pp. 898-911, 2007.

45. Jordan, J., K. I. Jacob, R. Tannenbaum, M. A. Sharaf, I. Jasiuk, "Experimental Trends in Polymer Nanocomposites – A Review", *Mater. Sci. and Eng.*, A 393, pp. 1-11, 2005.

46. ISO R527-1966 (E), "Plastics – Determination of Tensile Properties", International Organization for Standardization, 1966.

47. ISO 178-1975 (E), "Plastics – Determination of Flexural Properties of Rigid Plastics", International Organization for Standardization, 1975.

48. ISO 180-1982 (E), "Plastics – Determination of Izod Impact Strength of Rigid Materials", International Organization for Standardization, 1982.